SAND79-8280
Unlimited Release

UC-62c

Design, Cost and Performance Comparisons of Several Solar Thermal Systems For Process Heat

Volume II: Concentrators

E. D. Eason

Prepared by Sandia Laboratories, Albuquerque, New Mexico 87115
and Livermore, California 94550 for the United States Department
of Energy under Contract DE-AC04-76DP00789.

Printed March 1981

Sandia Laboratories
energy report

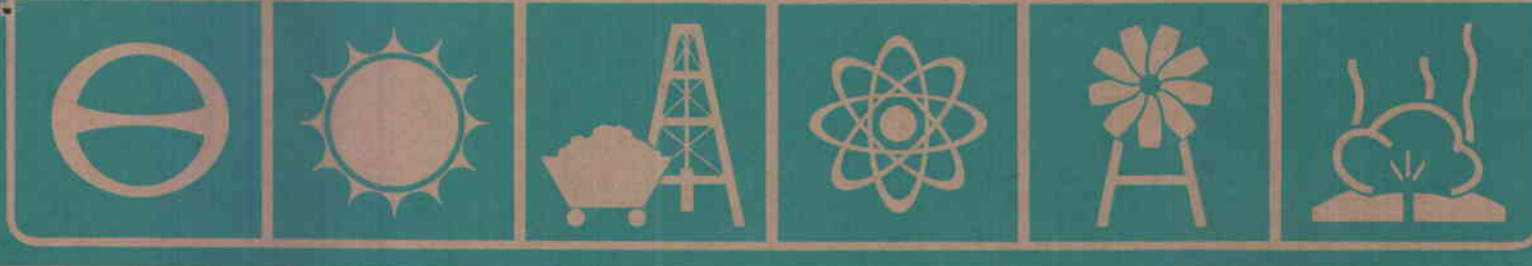

SF 2900-QQB(3-74)

Issued by Sandia National Laboratories, operated for the United States Department of Energy by Sandia Corporation.

NOTICE

SAND79-8280
Unlimited Release
Printed March 1981

UC-62c

DESIGN, COST AND PERFORMANCE COMPARISONS OF SEVERAL SOLAR THERMAL SYSTEMS FOR PROCESS HEAT

VOLUME II: CONCENTRATORS

Ernest D. Eason*
Energy Systems Studies Division
Sandia National Laboratories
Livermore, California

ABSTRACT

This portion of the comparison study identifies the major mechanical design and cost differences between concentrator subsystems. Parabolic dishes and troughs are designed to the same specifications as heliostats, using the same glass mirror/steel structure design concept and their costs are estimated on a consistent, comparable basis, using the heliostat cost data base. The results show inherent cost differences arising from differences in geometry, the cost of providing curvature and wind loadings. The estimated cost increases, relative to heliostats, are 15% to 50% for dishes and 0% to 30% for troughs, considering the combined effect of several analysis uncertainties. The concentrator cost estimates are used in the systems analysis volume (Volume V) to obtain cost/performance estimates for the overall systems.

*Now with Failure Analysis Associates; Palo Alto, California.

ACKNOWLEDGMENTS

The author appreciates the data, advice, and insights provided by people too numerous to name at the Jet Propulsion Laboratory, Sandia National Laboratories, Solar Energy Research Institute, and their contractors. Acknowledgment of their kind assistance should not be construed as implying that the program managers of the parabolic trough and dish programs have approved the results of this study.

CONTENTS

ILLUSTRATIONS

TABLES

DESIGN, COST AND PERFORMANCE COMPARISONS OF SEVERAL SOLAR THERMAL SYSTEMS FOR PROCESS HEAT

VOLUME II: CONCENTRATORS

1.0 Introduction and Summary

The application of solar thermal technologies to production of heat for agricultural and industrial processes has received increased attention in the Department of Energy's solar program during the last several years. Because of the relative newness of this interest no analysis to date has compared the potential cost and performance (in other words the energy cost) of the various solar thermal technologies as producers of process heat. There have been a number of comparisons of solar thermal technologies in electric power production (1-1 through 1-5 for example); but, for several reasons, there is no assurance that rankings which are obtained from those studies will apply to thermal applications. The main purpose of the study discussed here and in the accompanying volumes (1-6 through 1-9) is to make an initial cost and performance comparison of a number of the potential technologies which could be used for production of process heat. As is discussed in (1-6) the comparison made in this study is between systems using parabolic trough, parabolic dish or central receiver technology.

Any high-temperature solar collector requires a concentrator. The concentrator includes all the reflective surface, structure, foundation, tracking, and associated equipment needed to capture light from the sun, concentrate it, and redirect it to a useful location. At that location, the receiver subsystem converts the light into heat. By definition, the concentrator cost will exclude the receiver and portions of the system that support the receiver or its associated piping, though those parts are designed (in Appendix A) as an integrated part of the concentrator structure.

The purpose of this study is to examine the inherent design and cost differences in concentrator technologies. The most obvious approach to this task is to compare existing designs for each technology. However, each technology has evolved relatively independently, accepting different performance standards, assuming different environments, and using different materials, production methods, manufacturing volumes, and cost estimating techniques. Perhaps of equal importance, the heliostat and trough technologies have been under active development longer than dishes, so any comparison would be between production heliostat and trough designs and early conceptual and prototype dish designs. Under such circumstances, a comparison is more likely to identify differences in methodology and state of development rather than inherent differences in technologies.

A second approach is to design completely new versions of all three technologies, using consistent specifications, design methods, and costing procedures. This approach puts all technologies on the same conceptual design level, removes much of the cost estimating bias, and ensures that the designs will all survive in the same environment. However, there is never any assurance that the new conceptual design for any technology is close to the optimum configuration for that technology.

The approach taken here is to accept the specifications, design concept, and cost data for one technology (heliostats) and create conceptual designs for the other two, based on the same concept, designed to similar stresses and strains in equivalent environments, and capable of similar structural and tracking performance. Unlike the first approach, the designs are functionally comparable and consistently analyzed and costed. Unlike the second approach, at least one design is relatively mature, and the inherent differences are evident when that mature concept is transferred to the other configurations. The primary potential source of bias is the assumption that the heliostat design concepts can be transferred to dish and trough applications without major cost increases. This approach was selected because it provides insight on the inherent differences and reasonably comparable costs, and the conceptual bias is clear and easily understood.

Significant differences between concentrators are evident. The curved shape and greater distance between the center of pressure and the drive axis leads to greater drive moments on the dish than the heliostat. The same factors tend to increase the drive moment on the troughs as well, and the large aspect ratio increases the wind loads further, but a smaller characteristic length results in a lower drive moment for troughs than for the other two designs. These differences in wind loadings in turn cause the drive costs, structural weight, and pedestal designs to be significantly different.

There are also fundamental geometric differences. The dish is inherently r-θ geometry, compared to the x-y geometry of the heliostat. Thus, support spacings vary with r, and the structural efficiency of the dish is lower. The large aspect ratio of the trough requires more pedestals per unit area than for dishes or heliostats, so the pedestal/foundation costs are higher and a stiff structure is required for support between the pedestals. Both dish and trough designs have inherently more costly mirror surfaces than heliostats, both because of greater surface area per unit aperture and because of the greater cost of producing the curved surfaces.

The net effect of all identified differences is a modest difference in the costs of the three concentrators. The expected costs, under several assumptions discussed in following sections, are \$66/m^2 for heliostats, \$75/m^2 for troughs, and \$86/m^2 for dishes. All costs are in 1979 dollars, and all areas are net aperture area for a nominal 50 m^2 design. Because of the comparative estimating approach, the incremental costs of troughs and dishes over heliostats are expected to be approximately 15% and 30%, respectively, regardless of the absolute accuracy of the cost estimates.

The sensitivity of these cost estimates to changes in several assumptions is investigated. Variations in component scaling laws, wind force and moment coefficients, curvature penalties, and concentrator size are considered, as well as alternate concepts. Several individual sources of uncertainty are

combined to estimate an overall uncertainty in the $/m^2 figures given above; the ranges are +14%, -12% for dishes and +13%, -10% for troughs. Dishes and troughs over a broad range of sizes and with several alternate design concepts are expected to fall within these cost ranges.

2.0 Design and Cost Estimating Methodology

The comparative design and cost methodology is shown schematically in Figure 2.1. Consistent design concepts and identical analysis approaches combine to produce designs with equal structural performance and strength. The same operating environment (wind speeds, soil, etc.) is assumed in all calculations during the design process. These comparable designs are then combined with a uniform cost estimating procedure to generate costs that can be directly compared. The relative values of cost are fairly accurate, because all cost differences are based on identified design differences.

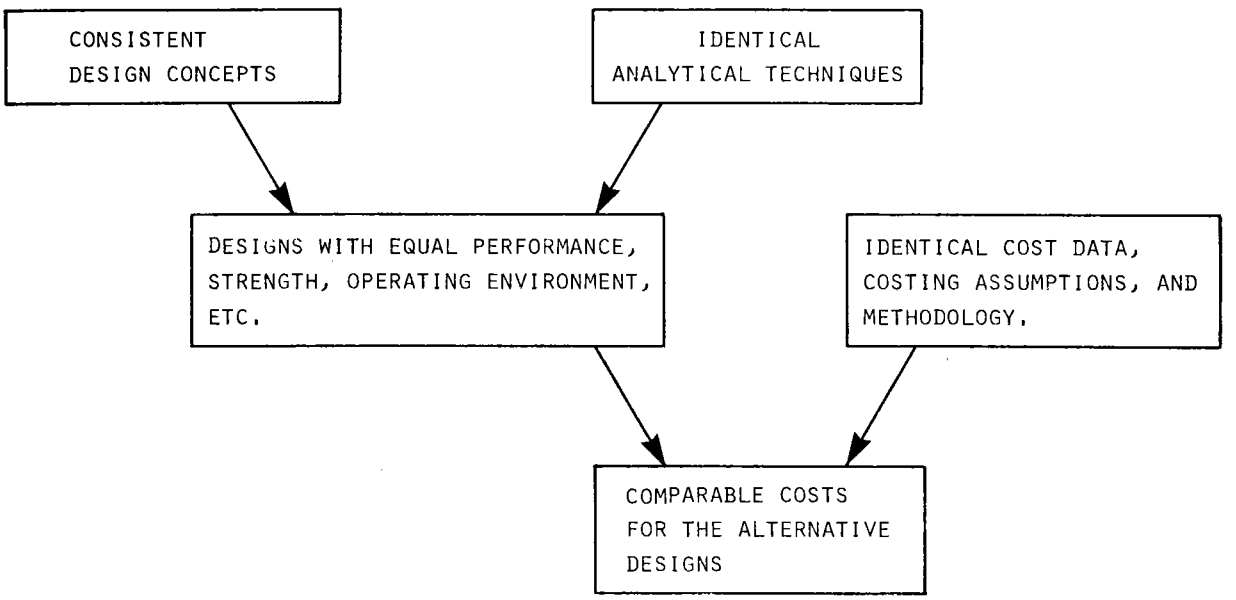

Figure 2.1. Comparative Design and Costing Methodology

The key assumption underlying this approach is that the best design concept for heliostats is equally applicable to troughs and dishes. For instance, the highest performance mirror concept, the lowest cost pedestal concept, and the same type of drives are applied to all three concentrators. This assumption breaks down only if the design concept cannot be transferred without a large cost increase. In that case, some competing concept that is more expensive than the optimum heliostat concept when applied to heliostats may be less expensive than transferring the heliostat concept to the dish or trough. The laminated glass mirror is an example where this may occur; it remains to be proven that accurately curved laminated glass mirrors can be

produced for only 5% higher cost than flat glass, as assumed here. The assumption that this can be done is favorable to trough and dish designs, because the laminated glass mirrors are less expensive and have higher performance than the polished aluminum and coated mylar surfaces that were used on dish and trough prototypes.

An important feature of the present approach is the use of consistent analytical techniques for comparative design. In practice, this means that the heliostat structural design is accepted as adequate for the identified loadings, the differences in loading between heliostat and dish or trough are identified, and the relevant members in the dish or trough are sized to withstand the loads with approximately the same stresses and deflections as in the heliostat. A detailed structural analysis is outside the scope of this project, so the dish and trough designs are based on strength of materials analytical approaches.

There is a hidden assumption in designing to equal deflections, namely that the losses due to structural deflection should be comparable for the different technologies. This is probably valid to first approximation for concentrators that produce the same concentration ratios, but perhaps designs with lower concentration ratios can tolerate greater structural error. Cost reduction from greater flexibility in the trough design is analyzed in Appendix B, but overall this is a cost/performance trade-off issue and the corresponding performance penalty is not yet known.

An additional assumption is that none of the concentrators needs to invert for wind, hail, or dust protection. Recent results for heliostats indicate that this is the case (2-1), and the same conclusion should hold for the dish and trough designs presented here, since they share the same mirror and structural design, as well as a similar washing scenario. The issue is not fully resolved, but this assumption is favorable to dishes and heliostats, because an inverted stow capability for those concentrators would require an additional drive component. All three designs suffer some performance degradation and require additional structural support and land area per unit aperture area if they stow inverted.

There are many other design concept and analysis assumptions which are discussed where used in Appendix A. Several important assumptions are checked for their effect on cost in Section 4 and Appendix B. Where uncertainties remain, an attempt has been made to resolve them in favor of the dish and trough designs, as in the small cost penalty for curved mirrors and the low cost assumed for the dish hub.

The basic structural costing methodology is to estimate the amount of material required for equal strength and performance of all major cost items. Since the same section shapes are used (except for dimensions) and the parts have the same function and method of manufacture and assembly, the cost per pound for these items is assumed to be the same. This cost per pound includes labor and materials, contingency and fee, and it is calculated from the heliostat weights and costs on an item-by-item basis. This approach implicitly accounts for design details such as fasteners, brackets, etc. The validity of dollar-per-pound scaling is discussed in Section 4.1.

A single source of detailed cost and weight information is conveniently available in (2-2) for all components of the glass mirror/steel structure heliostat design concept. These cost data are based on established production at 25000 units (13 million sq. ft.) per year, a much higher production rate than is assumed by most available cost estimates for dishes and troughs. Capital costs for the production plant and equipment are not included in the data, but these costs are estimated at less than 10%. In all cases, 10% contingency and 8% fee (profit) are included in the estimates, and the data are adjusted to 1979 dollars by adding 10% to the data which is in 1978 dollars.

The cost of the drives is scaled from the heliostat data, using a power function scaling rule (see Appendix A, Section A.4.) The mirror surface cost is based on differences in surface area per unit aperture arising from curvature and an assumed extra cost for producing the curved panels. The details are given in Section A.3. Other costs, for instance installation, controls, and wiring, were estimated from the heliostat data by identifying the inherent design differences and estimating the cost differential. The details are given in Section A.6. The sensitivity of total cost to errors in the estimates for each of these categories is discussed in Section 4.1.

The pedestal design used here differs from the previous heliostat pedestal. It was, therefore, necessary to develop an approximate bottom-up cost estimate for pedestals for all three concentrators. The necessary dimensions for withstanding wind loads were calculated, establishing the amount of material required and material cost. Labor costs and miscellaneous costs such as the electrical box were taken from (2-2) and other sources discussed in Section A.5. It should be noted that the comparative cost estimates are considered accurate enough for use here, but the pedestal designs are still at an early conceptual stage.

3.0 Baseline Results

The designs resulting from this study are shown in Figures 3.1 through 3.3. Additional detail for the parabolic dish is presented in Appendix A, Figure A.4. Complete dimensions and detail drawings for the heliostat design are presented in Reference 3-1.

All three designs feature laminated glass mirrors which are bonded to steel hat-section supports. These are bolted to channel-section beams, except for the trough, where they attach directly to the main beam or torque tube. For the dish and heliostat, the channel section beams attach to a main beam or hub with circular cross section. The drives connecting main beam and pedestal are harmonic drives as detailed in (3-1) for greater than 90° motion, and screw jacks for 90° or less. The drives bolt to the top of a hollow, pre-cast, prestressed concrete pile, which is driven in place in the field with conventional high-accuracy pile driving techniques.

The primary design consideration is the effect of wind loads on stresses and deflections. Table 3.1 summarizes the detailed wind load analysis in Appendix A. It is apparent that the maximum lift and drag forces are similar,

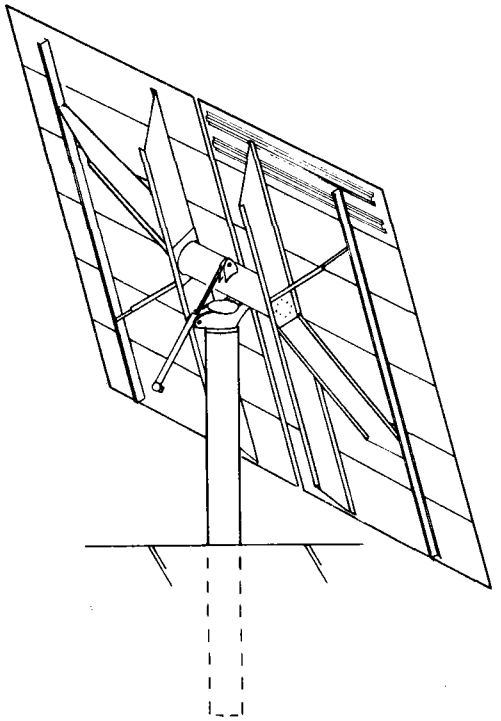

Figure 3.1. Heliostat

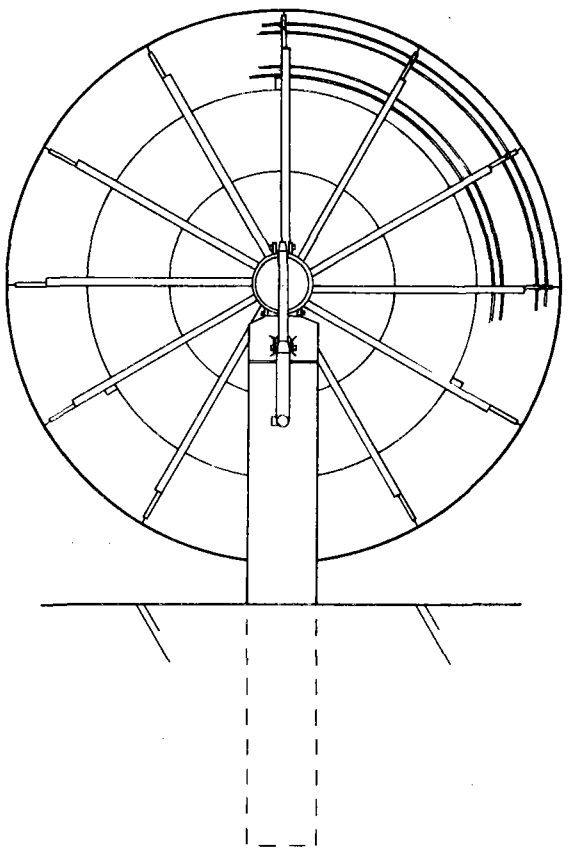

Figure 3.2. Parabolic Dish, Rear View

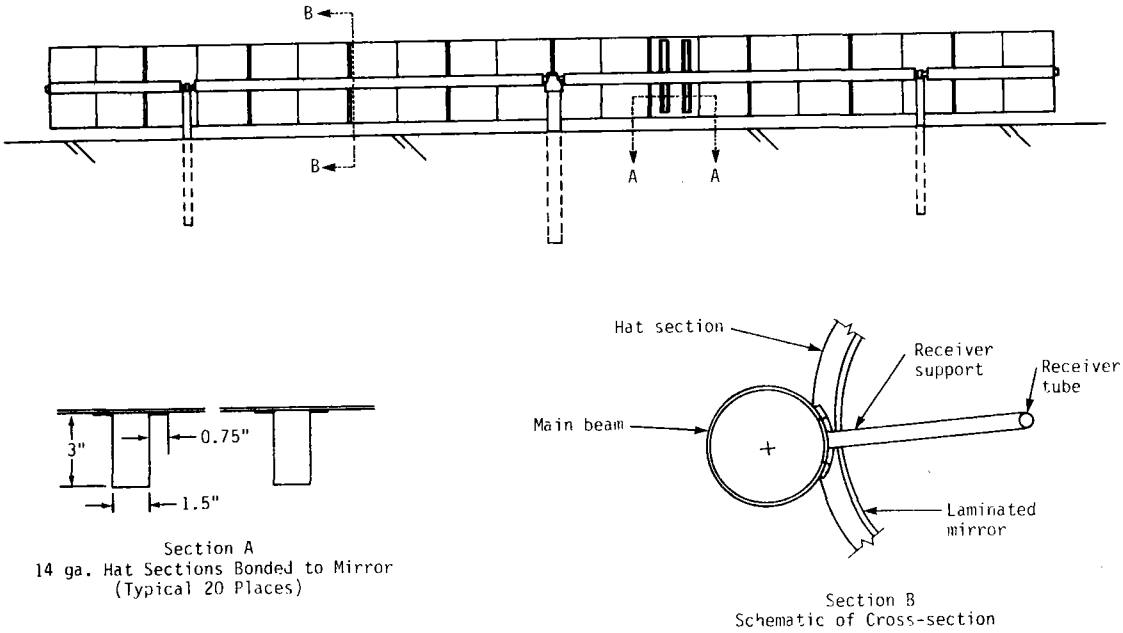

Figure 3.3 Parabolic Trough, Rear View

but they act at different distances from the axes so that the moments vary by a factor of 3.3. This large difference in elevation drive moment has a significant effect on structural design and required drive capacity.

TABLE 3.1

SUMMARY OF WIND LOADS

Maximum load at Drive Axis	Dish	Heliostat	Trough
Lift Force, lb	3800	3800	3600
Drag Force, lb	3900	3200	3800
Elevation Moment, lb-ft	43000	24200	13200
Azimuth Moment, lb-ft	11700	8800	-

Table 3.2 summarizes the differences in the weight of similar components in dishes, troughs, and heliostats. The glass weights depend only on the surface areas. Drive weight is scaled to output torque requirements. Structural weight reflects the effect of wind loads except in the case of the troughs, where the weight of the trough and distance between pedestal supports

are major factors in the main beam weight. The hat sections for the trough weigh more than for the heliostat or dish because they have been strengthened to eliminate the need for support beams. The pedestal weights vary primarily because of differences in wind loads, but the three trough pedestals are almost as heavy as the single heliostat pedestal (which carries twice the moment) because larger pedestals are more efficient. This is because strength of the pedestal is roughly proportional to (diameter)^3 while area increases as (diameter)^2.

TABLE 3.2

WEIGHT BREAKDOWN FOR DISHES, TROUGHS, AND HELIOSTATS

	Dish	Trough (N-S)	Heliostat
Mirrors			
Glass Weight, lb	1927	2041	1785
(Surface Area, ft^2)	(570)	(604)	(528)
Drives			
Elevation, lb	126		80
Azimuth, lb	513	563	407
Subtotal, lb	639	563	487
Structure			
Hat Sections, lb	370	674	336
Support Beams, lb	1547	-	698
Main Beam or Hub, lb	200	750	233
Subtotal, lb	2117	1424	1267
Pedestal/Foundation			
Steel, lb	560	359	368
Concrete, lb	5600	2941	3550
Subtotal, lb	6160	3300	3918

Table 3.3 summarizes the costs for the three concentrators, broken down into component categories. The detailed cost calculations are in the corresponding section of Appendix A.

The cost categories require some definitions. Mirror Surface includes only the laminated glass mirror. The major cost drivers are the glass surface area, which is greater for the curved designs, and the 5% manufacturing cost penalty assumed for curved glass. The Drives category includes the motors, gears, screws, bearings, and housings. There are both azimuth and elevation drives for dishes and heliostats, but only a single drive for the troughs. The major cost driver is wind-induced output torque requirement. Controls and Wiring includes a central field computer, local microprocessors, field wiring (including installation), and motor controllers. The major cost drivers are simpler local controllers in dishes and troughs and only one motor requiring power and a controller in the trough. Structure includes steel hat sections, support beams (if any), and a main beam or central hub. Curved

TABLE 3.3

COST BREAKDOWN FOR DISHES, HELIOSTATS, AND TROUGHS, 1979$

	Dish	Heliostat	Trough (N-S)
Mirror Surface	$ 643	$ 566	$ 680
Drives	1209	868	698
Controls and Wiring	309	381	213
Structure	934	553	708
Pedestal/Foundation	677	498	746
Installation and Other	453	358	527
Total $/Unit	$4225	$3224	$3572
Total $/$m^2$ Aperture	$86/$m^2$	$66/$m^2$	$75/$m^2$
Active Aperture Area	49.3m^2	49.1m^2	47.5m^2

Note: Costs assume established production at 25000 units per year, including 8% fee and 10% contingency, but excluding production facility capital costs. "Other" includes checkout, assembly, maintenance equipment and transportation (except pedestal), but not land, receivers, or piping. The $/$m^2$ figures are based on active aperture area.

members in dishes and troughs are estimated at 5% above the cost of the straight members in the heliostat. The main cost drivers are wind loadings and geometry. Pedestal/Foundation includes the cost of materials and factory labor, field surveying and installation (pile driving), and shipping 500 mi. The major cost drivers are wind loading and shipping weight. There is a large constant per-pedestal cost, including factory labor, surveying, setup for driving pedestals, and moving between locations. That is why the three pedestals for a trough cost more than the single dish or heliostat pedestal (see Table 3.3) even though they weigh less (see Table 3.2). Installation and other includes checkout, assembly (of mirrors to drives to pedestal), miscellaneous equipment and spares, and shipping all but the pedestal 500 miles. The major cost drivers are installation time and shipping weight.

As noted below Table 3.3, these cost estimates are based on volume production, and they include a modest fee or profit (8%) and contingency (10%). The cost of land, receivers and receiver supports, and piping are not included. These designs were all sized to provide roughly 50 m^2 of aperture area. However, part of the dish and trough surface is inactive, because it is always shadowed by the receiver and receiver supports. The active aperture area used in calculating $/$m^2$ is noted for reference in Table 3.3.

The relative accuracy of these comparative estimates is evaluated in the sensitivity studies which follow. The absolute accuracy can only be evaluated by detailed checking of the basic data, comparison with other items and typical development experience, and independent estimates. This has been done for heliostats (3-2) - (3-4), and when the results are consistently stated, the agreement between independent estimates is reasonably good. The $\$66/m^2$ heliostat cost listed in Table 3.3 is below the estimates in (3-2) - (3-4) primarily because a 20% cost reduction results from elimination of inverted stow capability and use of the one-piece pile pedestal/foundation concept.

4.0 Discussion of Sensitivity Studies

Many uncertainties remain in the comparative cost estimates, because of the immaturity of the dish and trough designs and the use of scaling laws and assumptions in the cost estimates. The effect of these uncertainties on total cost is estimated in the following section. In addition, fundamental assumptions about optimum concentrator size are analyzed, and the merits of competing design concepts are discussed.

4.1 Effect of Uncertainties in the Baseline Results

Consider first the effect of assuming different cost penalties for the curved surfaces. If there is no cost penalty, the costs for dish and trough mirrors drop by \$31 and \$32 and their structural costs drop by \$40 and \$16, respectively. These effects are -1.7% and -1.3% of the total cost for dishes and troughs, respectively. Similarly, a 10% cost penalty on all curved items would increase the total costs of dishes and troughs by less than 2%. A reasonable upper bound on the effect of curvature is to assume that the cost of sagged glass is about 50% above the flat mirror cost*, but that the cost of the curved steel members is only 10% above the straight member cost. The result is that total dish and trough costs increase by \$311 and \$303, or 7.4% and 8.5%, respectively.

A second uncertainty is the drive cost scaling law. The exponent $n = 0.8$ was used for baseline results, but the credible range is large, as described in Appendix A, Section A.4. If the drive cost increases linearly with torque ($n = 1$), the drives cost an additional \$108 and \$61 for dish and trough, respectively. These increases are 2.6% and 1.7% of the total costs for dishes and troughs. If the exponent is $n = 0.4$ (the value found for hydraulic drives), the costs would decrease by \$187 and \$103 for dishes and troughs. These changes are 4.4% and 2.9% of the dish and trough total costs.

A third uncertainty is the use of \$/lb for structural cost scaling. The labor cost does not necessarily increase with component weight, and labor is included in the \$/lb figure. However, the fraction of labor in the structural components is small, i.e., 10% of support beam cost and 23% of main beam cost. Most of this labor is for assembly, divided between support beam assembly

*The actual cost penalty is currently under study at Sandia National Laboratories, Albuquerque.

(glass, hat sections, and beams) and main beam assembly (main beam, end plates, and attachment to drives). The hat sections are a purchased part, with an unknown amount of supplier labor included. The structural weight of dishes and troughs exceeds that of heliostats (see Table 3.2), so the labor cost has been increased by the $/lb scaling rule.

The magnitude of the increase can be estimated by assuming the same labor for dishes and troughs as for heliostats and noting the effect on total costs. Assume 20% of the hat section cost quote is labor, yielding the same 37¢/lb raw material cost as the support and main beams. The total structural labor costs are $32 and $65 higher for dishes and troughs than for heliostats, or 0.8% and 1.8% of the total costs, respectively. This calculation was performed on the costs before adding curvature penalties, so the $/lb effect is independent of the curvature penalty effect. The results are clearly an overestimate of the effect of $/lb scaling, because there are differences which should lead to greater labor costs, such as heavier individual pieces (particularly trough main beam), greater numbers of dish support beams (12 vs. 8 in heliostat), and more hat section pieces (72 in dishes, 40 in troughs, and 24 in heliostats).

There are substantial uncertainties in the wind force and moment coefficients, arising from disagreement between experimental data, incomplete data, wind tunnel modeling uncertainties, and the possible effect of wind fences. The effect of wind fences is small in the stowed position, and the effect on elevation moment (for troughs, at least) is small in operating and stow orientations (4-1). This is a significant finding, because elevation moment is related to the wind forces that determine the size of support beams, main beam, and drives, and affect the pedestal design, as well. Wind fence effects are lumped with all other uncertainties in wind coefficients, and a reasonably wide range ($\pm$25%) in those coefficients is considered. The elevation moment coefficient for the dish at the -25% bound is equal to that of the heliostat, and at the +25% bound, it approaches that of the trough.

The detailed effect on dish and trough design of a $\pm$25% variation in all wind coefficients is analyzed in Appendix B. The primary effects are on support beams in the dish, hat sections and main beam in the trough, and drives and pedestal for both concentrators. The effects are quantified by the use of scaling rules, obtained by fitting a power function to the several point designs developed for each component in the course of this study (see Section B.4). The result is that a $\pm$25% variation in wind coefficients leads to a $\pm$10% variation in total dish cost, and a $\pm$9% variation in total trough cost.

The four uncertainties discussed above affect most of the cost categories listed in Table 3.3 The curvature cost penalty affects mirror surface and structural costs for hat sections and support beams. The uncertainty in drive cost scaling affects the Drives category. The $/lb scaling affects all portions of structure, independent of the curvature penalty. Finally, the uncertainty in wind coefficients affects the categories Drives, Structure, and Pedestal, again independent of the other uncertainties. The only categories that have escaped sensitivity analysis to this point are Controls and Wiring and Installation and Other. Together these categories account for only 18% of dish cost and 21% of trough cost. If the estimates in these categories are off by +20%, the resulting effects on total dish and trough cost are only 3.6% and 4.1%, respectively.

The effect of all the uncertainties considered above can be combined into a single measure of the uncertainty in the dish and trough costs. Assuming the uncertainties are independent random variables, the appropriate method for combining them to form probable founds is to sum the squares of the percentage effects and take the square root (RSS). The results are given in Table 4.1. Assuming the heliostat cost data is accurate, the probable uncertainty in the comparative dish and trough cost estimates is ±14%, -12% for dish cost, and +13%, -10% for trough cost. Applying these uncertainties to the $\$/m^2$ data in Table 3.3, the cost of dishes is estimated at 15% to 48% higher than heliostats, and the cost of troughs is 2% to 28% higher than heliostats.

TABLE 4.1

COMBINED EFFECT OF UNCERTAINTIES IN COMPARATIVE COST ESTIMATES

Source of Uncertainty	Effect on Total Cost			
	Dish		Trough	
Curvature Cost Penalty (Range: None to 10% Structure, 50% Glass)	+7.4%	-1.7%	+8.5%	-1.3%
Drive Cost Scaling Exponent (Range: 0.4 to 1.0)	+2.6	-4.4	+1.7	-2.9
$/lb Structure Cost Scaling (Effect of Same Labor Cost as Heliostat)	-	-0.8	-	-1.8
Wind Coefficients (Range: ±25%)	+10.4	-10.4	+8.6	-8.6
Assumptions in Installation, Other, Control and Wiring Cost Categories (Range: ±20%)	+3.6	-3.6	+4.1	-4.1
Combined Effect on Cost $(\Sigma(\%)^2)^{1/2}$ =	+13.5%	-12.0%	+12.9%	-10.2%

4.2 Effect of Variation in Trough and Dish Size

The sensitivity of trough cost to trough length is shown in Figure 4.1. The basic approach was to generate point designs for several lengths using simplified analyses and cost scaling laws for wiring, drives, and pedestals. The calculations and results are described in detail in Appendix B. The fundamental effects are: mirror surface and hat section costs increase directly with trough length, the main beam cost increases faster than trough length, and all other cost components increase more slowly than trough length.

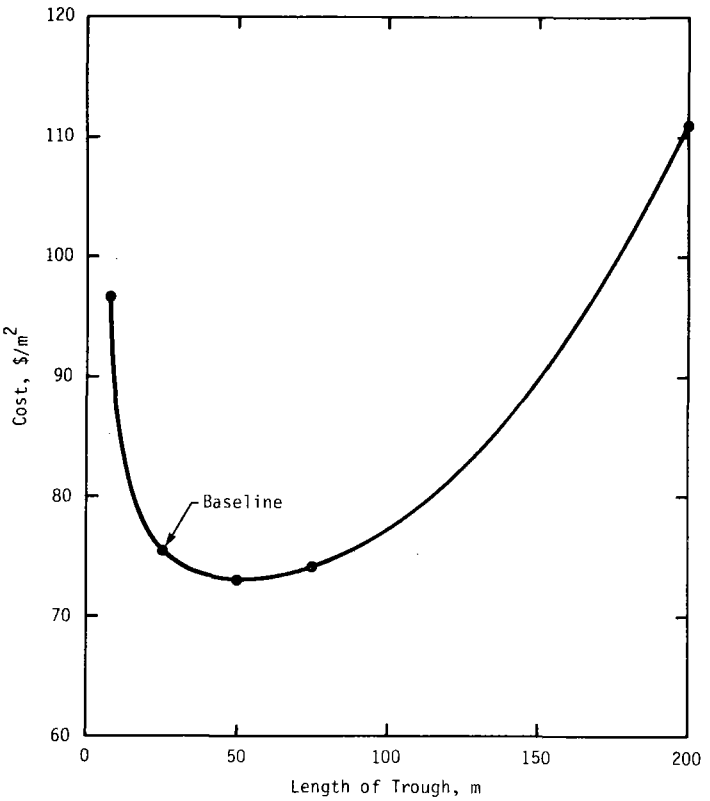

Figure 4.1. Sensitivity of Trough Cost to Length of Trough per Drive

It is apparent from Figure 4.1 that the 25 m baseline trough is somewhat shorter than optimum, but over the range of lengths 25-75 m, the cost varies by only about 3%. This is within the accuracy of the scaling and redesign procedure, particularly since the changes in total cost arise from partially compensating component cost changes. The 25 m trough is, therefore, accepted as close to the optimal length. For a similar 2 m wide trough, the optimal length was independently determined as 24 m (4-1).

The effect of $/lb scaling is much greater for longer troughs than for the baseline results discussed above. This is because the major cost component in longer troughs is the main beam (see Table B.2), and the $/lb figure applied to that cost includes 23% labor. Labor costs undoubtedly do increase with trough length, because the longer beams are made in more sections and they are heavier and more difficult to fabricate and handle. If one assumes that labor costs are proportional to length, rather than weight, the total costs in Table B.2 and Figure 4.1 decrease by 2%, 4%, and 11% for 50 m, 75 m, and 200 m troughs, respectively.

The effect of wider troughs is also considered, as detailed in Appendix B, Section B.2.2. For a trough that is twice as wide, the wind moment increases by a factor of about five. The greater wind loading requires relatively deep support beams in place of hat sections, a higher capacity drive, a stiffer main beam, and stronger pedestals. The net effect is an $\$85/m^2$ trough--a diseconomy of scale--whereas a trough that is twice as long shows an economy of scale. The primary reason is the fact that wind moment varies as $(\text{width})^{2.3}$ and drag force varies as $(\text{width})^{1.3}$, but both loads vary as $(\text{length})^{1.0}$.

There is clearly an incentive to increase trough area by increasing length rather than width.

In the Energy Centralization portion of this study (Volume IV), larger dishes are shown to result in lower piping costs. To determine the overall advantage or disadvantage to larger dishes, it is necessary to estimate the effect of size on concentrator costs. The approach taken is to generate point designs at various sizes, using scaling rules and simplified redesign rules. The calculations and results are described in detail in Appendix B, Section B.1. The basic effects are: mirror surface scales with aperture area, drive and structure cost increase faster than area, and all other categories increase more slowly than area. The total effect is a diseconomy of scale, as shown in Figure 4.2. Dishes smaller than 20 m^2 were not considered because of the excessive energy centralization cost. However, published preliminary results for small dishes, (4-2), show increasing costs per aperture area as each of several dish designs is reduced in size.

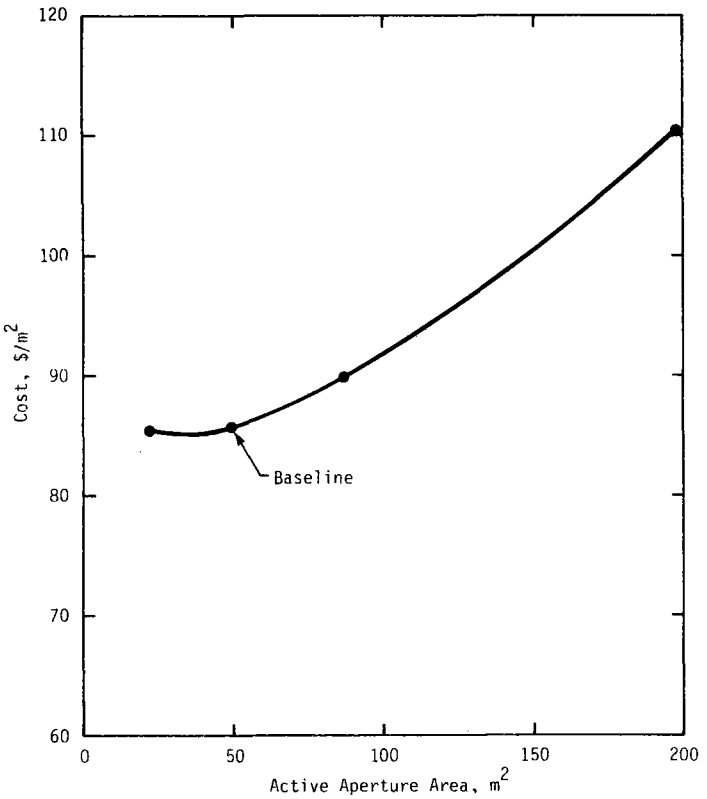

Figure 4.2. Sensitivity of Dish Cost to Aperture Area

The effect of $/lb scaling on dish cost increases as size increases. To bound the effect, assume that the labor cost for hat sections, support beams, and main hub is independent of size. This would result in a 5% increase for the 22.4 m^2 dish, and 2% and 4% decreases for the 87 m^2 and 198 m^2 dish total costs as given in Table B.1 and Figure 4.2. This is an overestimate of the $/lb effect, because in fact the labor costs do vary with size. With larger dishes, there are more pieces, and there are fabrication and handling difficulties because the pieces are larger.

4.3 Discussion of Alternate Design Concepts

The lower concentration ratio of the trough compared to dishes and heliostat fields may imply a greater tolerance of structural error. To investigate the value of a more flexible trough, an alternate design was generated (see Appendix B, Section B.3). The approach was to relax the deflection requirements and design a trough that is stress and buckling constrained. For 47.5 m^2 active aperture, the best result is a two-pedestal design with 3-10 times greater deflections than the baseline design. The resulting cost reduction is 12%, which makes the north-south trough cost equal to the heliostat cost ($66/$m^2$). The cost can be further reduced by simultaneously increasing the area to 74.4 m^2. With the same maximum deflections, the cost decreases an additional 4% for the longer trough, to $63/$m^2$.

Greater flexibility causes a performance penalty, which has not been evaluated. The necessary (breakeven) cost reduction for justifying more flexible heliostats has previously been investigated (4-3). The cost-effectiveness of a more flexible trough or dish cannot be assessed without similar detailed performance calculations. In addition, it is possible that the stiffness of both dishes and heliostats could be relaxed somewhat, affecting the relative comparison. The relative cost of dish, trough, and heliostat concentrators at individually optimized stiffness cannot be assessed without estimates of the cost reductions arising from more flexible dishes and heliostats. Intuitively, the longer, more flexible trough seems worthwhile. If the performance penalty is less than 5-10%, the effective cost of heliostats and troughs would not be significantly different.

Throughout this report, the troughs have been assumed to be installed with their length oriented north and south. An alternate concept is to install them east and west, which reduces the drive cost but increases the annual energy loss. The performance penalty is estimated in the Systems volume of this report as 12.5% loss in annual energy. The reduction in drive cost is $474 (13.3% of trough cost) if a screw jack with approximately 90° motion can be used in place of the azimuth-type drive. There would be a slight additional performance penalty due to inability to point north during early morning and late afternoon in the summer, but ignoring this, the question is whether a 13.3% reduction in trough cost justifies a 12.5% reduction in annual energy production.

The answer is evident from the fact that trough cost is only about 40% of the installed capital cost of a typical plant (see Executive Summary, this report). The plant capacity (and cost) would have to be increased about 12.5% to make up for the performance penalty, and the cost savings would be 13% of 40% of the total plant cost, or about 5%. Thus, an east-west orientation is not competitive with the north-south orientation.

The primary differences in design concept between the trough developed here and the current prototypes are: laminated glass mirrors instead of mylar or aluminum, open beam construction instead of monocoque, and fewer pedestals. The reasons why the new design concept is expected to reduce current costs are discussed below.

There is general agreement that some form of glass mirror is advantageous for both troughs and dishes, once low-cost techniques for curving glass are developed. The primary reasons are the greater performance and life of glass mirrors. If the production cost for reliably curving glass is as low as is assumed here, glass mirrors will surely be used. If not, trough (and dish) mirror costs will be higher than estimated here.

The currently used monocoque concept is partly justified by the need to supply a structural front skin to support mylar film, or by the use of the aluminum reflector as the front skin. With a laminated glass mirror, a front skin is not necessary, so the only issue is whether the monocoque design is the cheapest way to provide the necessary torsional and bending stiffness. As noted in Section B.2.1, monocoque construction makes sense for long troughs, but for the 25 m length considered here, a relatively small, thin, circular main beam provides sufficient stiffness with much less material. There is probably a length-dependent tradeoff between the two concepts, but that is outside the scope of this investigation.

The proper number of pedestals depends on a tradeoff between structural cost and pedestal cost. There is a high fixed cost per pedestal, plus attachment and alignment costs that increase with number of pedestals. Reducing these costs by increasing the distance between pedestals necessarily increases main beam cost. Two or three pedestals are sufficient for a 25 m length, and the beam stiffness that is required for reasonable torsional deflection over that length is sufficient to prevent unacceptable sag between supports. The major advantage to the large number of supports currently used is that the resulting trough sections are easily handled, interchangeable modules. However, the resulting total cost is higher than if fewer pedestals are used.

A variety of alternate dish concepts are currently under study. Two of these are a flattened segmented dish surface, analogous to a Fresnel lens, and a dish that is pivoted at the rim rather than the vertex. The principal advantage of these concepts is the expected reduction in wind moments, in the first case from making the dish look like a heliostat and in the second case from reducing the moment arm of the lift and drag forces. These designs are estimated to cost 5-16% more than heliostats, depending on size, based on preliminary evaluations (4-4).

The results developed here do not support such a small cost increment. This is demonstrated by assuming that the alternate design concepts completely eliminate the shape-related difference in wind moments between dishes and heliostats. This corresponds to a 25% reduction in the moment coefficient (see Tables A.1 and A.3), and the resulting effect on total dish cost is 10%, as calculated in Section B.4. Thus, if the alternate designs are totally effective in eliminating the inherent aerodynamic disadvantage of the dish, the cost would still be at least 130(0.9) - 100 = 17% higher than the heliostat cost. The important factors are the cost of producing curved surfaces, the moments caused by drag on receiver and struts, and the fact that gross aperture area, which affects wind loads, must be larger for dishes because of the receiver and strut shadows.

The cost increment for the Fresnel dish would probably exceed this lower bound. The moment coefficient should not decrease to the same value as the

heliostat, because the dish is necessarily thicker than a heliostat, and it presents curved surfaces to the wind. If the coefficient were reduced 15%, to $C_{me} = 0.13$, the dish would cost about 22% more than a heliostat. There would also be a cost increase arising from the greater number of structural and glass pieces in a Fresnel dish compared to the baseline dish.

A similar situation would occur for the edge-support concept. This concept was considered in early heliostat development and rejected as more expensive than the single pedestal concept. Thus, whatever the cost reduction due to moment reduction, there will be a compensating cost increase from the extra structure required for edge support. Depending on the relative magnitude of the cost reduction from moment reduction and the expected cost increases, the Fresnel and edge-supported concepts may be more or less expensive than the baseline concept presented here. Both are expected to fall in the same relative cost range as the baseline dish, 15% to 50% more expensive than heliostats for nominal 50 m^2 sizes.

An additional alternate dish concept is to enclose the dish inside a transparent, air-supported plastic dome. The dome would carry the wind loads and protect against hail damage, allowing a much less expensive mirror, structure, drives, and pedestal. The concept is under investigation for heliostats as well, but it is presently approximately 23% more expensive than the glass and steel concept (4-5), considering performance penalties, capital, O&M (washing), and land cost differences. It is not clear that the dome concept is cheaper than the glass and steel concept for dishes, but there are good reasons to believe that it is more likely to be cost-effective for dishes than for heliostats.

The primary factors in the effect of an enclosure are the transmissivity under average dirty conditions, the remaining structural requirement, given that wind loads are eliminated, and economies of scale, if any. The transmissivity for an optimally-washed enclosed heliostat is estimated as 0.67 (0.60 avg. net reflectivity $\div$ 0.89 mirror reflectivity, see Ref. (4-6)). For an optimally-washed enclosed dish, the transmissivity would be 0.82, because light would pass only once through the dome. Thus, the optical losses for an enclosed dish system would be at least 22% less than for an enclosed heliostat. In addition, the cost categories that are affected by the protection afforded by a dome (mirror, structure, drives, pedestal) account for a larger fraction of dish cost (82%) than heliostat cost (77%), so a slightly greater cost reduction is possible. These effects are partially balanced by the fact that the enclosed dish structure must be more expensive than an enclosed heliostat structure, because of the need to support the receiver. However, considering piping costs, the optimal dish size is probably greater than the optimal heliostat size (which is limited by receiver size, among other constraints), and the dome design might reduce the diseconomy of scale shown in Fig. 4.2. Considering all these factors, the enclosed dish appears to be an alternate concept that is worthy of detailed study.

5.0 Conclusions

Dish and trough concentrators appear to be 30% and 15% more expensive than heliostats, respectively, when they are comparatively designed and costed for approximately 50 m^2 aperture area. There are several uncertainties in these figures, including the effect of scaling rules on drive and structure costs, the cost of providing curved laminated glass and structural members, uncertainty in the wind coefficients, and uncertainty in various estimated installation, control, wiring, and other costs. These uncertainties are combined (by root-sum of squares) to estimate the uncertainty in the total cost of dishes and troughs relative to heliostats. Dishes are expected to cost 15 to 50% more than heliostts, while troughs may be comparable in cost or up to 30% more expensive than heliostats. The cost differences are primarily due to differences in wind loads, the cost of providing curvature, and geometric effects such as the inherent r-θ geometry of dishes and the large aspect ratio (12.5:1) of troughs.

The effect of size optimization on the relative cost is determined by scaling the baseline designs to other sizes. Wider troughs cost more per unit aperture, while longer troughs could be slightly (<5%) less expensive. The optimum length appears to be near 50 m. Increasing dish size increases the cost per unit aperture, but this may be a worthwhile system trade because the cost of piping decreases with increasing dish size.

Several alternate design concepts are discussed. Longer and more flexible troughs could have slightly (4%) lower cost per unit aperture than heliostats. The annual performance penalty is unknown, so the cost-effectiveness of this design change is uncertain. East-west orientation is not cost-effective compared to north-south, because the reduction in drive cost is more than offset by the resulting annual performance penalty. Alternate dish designs based on Fresnel and edge-support concepts are estimated to fall within the same cost range as the baseline dish, because the reduction in cost due to wind moment reduction is small (<10%) and partially offset by greater complexity and structural costs. Use of an enclosure appears more promising for dishes than for heliostats, and further investigation of the concept appears to be warranted.

These conclusions are based on a comparative design and costing approach, using data and specifications for a relatively mature heliostat concept. The sensitivity studies discussed in Section 4 and presented in Appendix B give confidence in the accuracy of the results. The expected cost ranges are generic in that they appear to be applicable to alternate concepts.

APPENDIX A--DETAILS OF MECHANICAL DESIGN AND COST ESTIMATES

A.1.0 Wind Load Calculations

The primary design loads for the three collectors are wind loads. There are four principal wind loads in any collector orientation: lift and drag forces, and torque about the elevation and azimuth axes. Both steady and unsteady (vortex) loads are generated by the wind, but for preliminary design, only the steady loads are considered. The loads enter the collector structure as pressure distributions on the mirror panels, resulting in flexure of the glass, steel hat sections, and support beams, and combined torsion and flexure in the main beam. The drives must withstand torques about each axis plus the vertical and lateral thrust of lift and drag. For this study, the drive output torque capacity must exceed the maximum wind torques, though the possibility of designing a locking device to carry those loads is acknowledged. The one-piece pedestal/foundation carries the loads from the drives to earth, in loading combinations that may include flexure (due to elevation torque and the moment of drag forces), torsion (from azimuthal torque), and axial tension or compression (the vector sum of collector weight and lift). Most collector costs are in some way influenced by the wind loads.

A consistent set of wind conditions has been defined for this study, based on heliostat specifications. In all cases, the maximum operating wind is assumed to be a 50 mph gust, which can come from any azimuthal direction with the collector in any orientation. The maximum survival load is 90 mph wind hitting the collector in its stowed position, with no more than 10° attack angle between the actual wind direction and the direction that would expose minimum area to the wind. Calculations verified that most loads are higher with 90 mph wind in stow position than with 50 mph wind in the worst-case operating orientation. The maximum steady wind speed for calculating operating deflections is 30 mph, in any direction and for any collector orientation.

Wind speeds are measured at a reference height thirty (30) feet off the ground. There is a boundary layer near the earth, resulting in lower wind velocities at lesser heights. The wind profile assumed for this study is

$$V(h) = V(30) \cdot (h/30)^{0.15} \qquad (A.1)$$

with height h measured in feet. This profile is given by several sources, for instance (A-1, A-2). For design purposes, h is measured to the highest leading edge of the collector when tipped 10° from face up (for survival

loads), or to the elevation axis (for operating loads). The effect of non-uniform velocity over the projected area is ignored. Check calculations show that loads calculated by the uniform assumption may be in error by about 5%.

In the preliminary design, the collectors are designed for stand-alone operation, ignoring any possible effect of wind fences. Preliminary data on heliostats indicates little advantage to wind fences, because the heliostat must be designed for the worst-case loads in stow position, and wind fences have only a minor effect on the loads in that orientation. In addition, the far-field heliostats are far apart, so that they provide negligible wind shadow for each other (A-2). Recent data show the effect of upstream troughs and wind fences on troughs (A-3, A-4), and that effect is again small for stowed troughs*, though it is significant at other attack angles. Based on this data, and the fact that worst-case loads occur in stow position, the effect of wind fences is considered in Section 4.1 as only one component of an assumed ± 25% overall uncertainty in force and moment coefficients.

The basic form of the equation for lift or drag force is

$$F = C\ A(\rho V^2/2) \tag{A.2}$$

where C is the lift (C_ℓ) or drag (C_d) coefficient. For moment due to wind,

$$M = C_m\ A\ L\ (\rho V^2/2) \tag{A.3}$$

where C_m is the moment coefficient. In both Eqs. (A.2) and (A.3), ρ is the air density (0.00238 slugs/ft^3), V is the wind velocity at height h (ft/s), A is the aperture area (ft^2), and L is a characteristic length (ft), equal to dish diameter, trough width, and heliostat mirror length or width (for elevation and azimuth moments, respectively). The coefficients C_ℓ, C_d, and C_m vary with the attack angle, defined here as the angle between the actual wind vector and the direction that would expose minimum cross section to the wind.

There is a relationship between lift and drag forces and moment, i.e.,

$$M_o = F_d a + F_\ell b \tag{A.4}$$

where a and b are the moment arms about the point o. In all cases, the point o for this study is the center of rotation of the drive, so M_o is the torque loading on the drive due to wind loads. Both the forces and the moment arms in Eq. (A.4) vary with attack angle. In practice, wind measurements on complex bodies are made in a wind tunnel by measuring forces and torques on a model with known areas and lengths, then calculating C_ℓ, C_d, and C_m from Eq. (A.2) and (A.3).

Tables of coefficients or loads as a function of attack angle are available in several sources (A-1)-(A-10). These were analyzed to determine the combinations of collector orientation and wind speed that would produce the worst-case

*Compare peak values of coefficients at $\theta = 90°$ in Figures 4 and 13 of Reference A-3.

loadings. For instance, the maximum drag on the dish occurs with the wind vector aligned with the axis of the dish, which can only occur up to 50 mph wind speed because the dish is in stow position at higher wind speeds. However, nearly the same drag load occurs in stow position, with 90 mph wind. The entire matrix of wind speeds and attack angles was evaluated. The resulting coefficient values are ported in Tables A.1 through A.3, together with the range of reported values (at the same orientation) and the sources of data. A sketch of each worst-case orientation considered in design is shown in Figures A.1 through A.3.

TABLE A.1

LIFT, DRAG, AND MOMENT COEFFICIENTS FOR HELIOSTATS

Condition, Wind Speed	Design Value	Reported Values and Source
Maximum Elevation Moment, Maximum Lift:		
Stowed, 90 mph, Fig. A.1(a)	$C_d = 0.14$	0.12 (A-5), 0.15 (A-6), 0.17 (A-7)
	$C_\ell = 0.42$	0.39 (A-5), 0.44 (A-6)
	$C_{me} = 0.11$	0.10 (A-2), (A-5), 0.13 (A-7)
Maximum Drag:		
Operating, 50 mph, Fig. A.1(b)	$C_d = 1.2$	1.2 (A-5), (A-6), 1.18 (A-8)
Maximum Azimuth Moment:		
Operating, 50 mph, Fig. A.1(c)	$C_{ma} = 0.15$	0.14 (A-2), (A-5), (Flat Plate)

Note: C_{me} and C_{ma} are elevation and azimuth moment coefficients. C_{me} is measured relative to the drive axis, assumed 1' below mirror surface.

TABLE A.2

LIFT, DRAG, AND MOMENT COEFFICIENTS FOR 12.5 ASPECT RATIO TROUGHS

Condition, Wind Speed	Design Value	Reported Values and Source
Maximum Positive Lift, Maximum Drag, Maximum Moment:		
Stowed, 90 mph, Fig. A.2(a)	$C_d = 0.50$	0.44, 0.54 (A-3)*
	$C_\ell = 0.50$	0.44, 0.85 (A-3)*
	$C_m = 0.27$	0.25, 0.29 (A-3)*
Maximum Negative Lift:		
Operating, 50 mph, Fig. A.2(b)	$C_\ell = -1.9$	-1.9 (A-3)*
Same, with Wind Fence	$C_\ell = -0.75$	-0.73 (A-3)*, -0.79 (A-9)
Specification:		
All Orientations for 3.75 Aspect Ratio and Wind Fence (A-9)	$C_d = 0.50$	
	$C_\ell = 0.50$	
	$C_m = 0.35$	

*These coefficients are the result of adjusting the values in Figure 4 of Reference A-3 to 12.5 aspect ratio using Figure 8 of Reference A-3.

TABLE A.3

LIFT, DRAG, AND MOMENT COEFFICIENTS FOR PARABOLIC DISHES

Condition, Wind Speed	Design Value	Reported Values and Source
Maximum Positive Lift, Maximum Elevation Moment:		
Stowed, 90 mph, Fig. A.3(a)	$C_d = 0.32$	0.25 (A-10), 0.46 (A-11)
	$C_\ell = 0.38$	0.38 (A-10), 0.38 (A-11)
	$C_{me} = 0.15$	0.10 (A-10), 0.22 (A-11)
Maximum Azimuth Moment:		
Operating, 50 mph, Fig. A.3(b)	$C_{ma} = 0.15$	Analogous to Elevation Moment
Maximum Drag:		
Operating, 50 mph, Fig. A.3(c)	$C_d = 1.42$	1.49 (A-10), 1.42 (A-12) 1.27 (A-6)

Note: C_{me} and C_{ma} are elevation and azimuth moment coefficients. C_{me} is measured relative to the drive axis, assumed 1' below mirror surface.

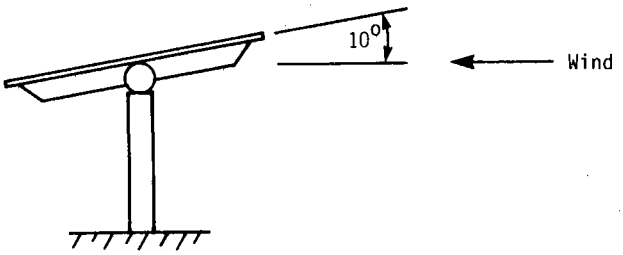

(a) Stowed, <10° Attack Angle, 90 mph Wind
(Maximum Elevation Mmoment, Maximum Lift)

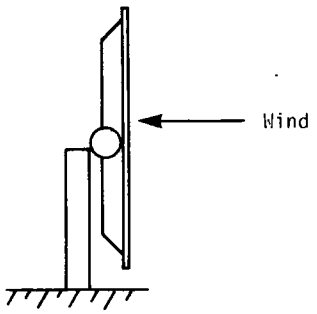

(b) Operating, Face into Wind, 50 mph
(Maximum Drag)

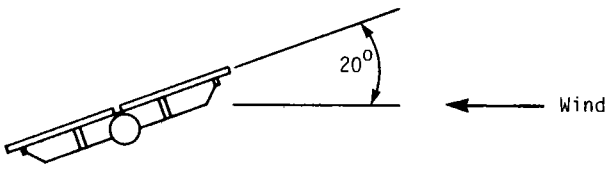

(c) Operating, Top View, 50 mph
(Maximum Azimuth Moment)

Figure A.1 - Orientations of Heliostat for Maximum Wind Loads

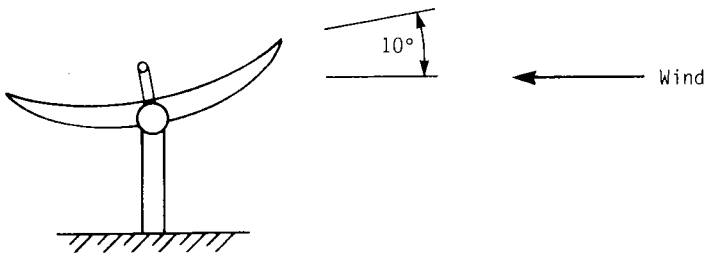

(a) Stowed, <10° Attack Angle, 90 mph Wind
(Maximum Positive Lift, Drag, and Drive Moment)

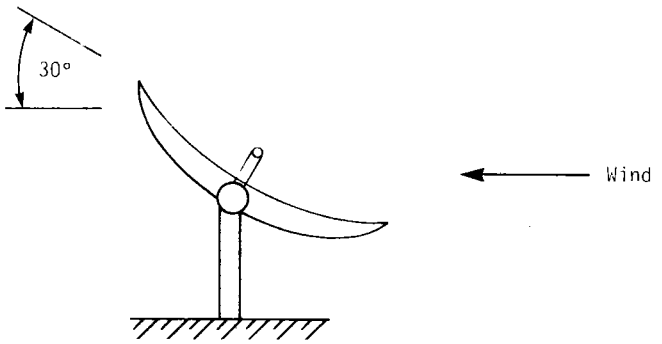

(b) Operating, 50 mph Wind
(Maximum Negative Lift)

Figure A.2 - Orientations of Trough for Maximum Wind Loads

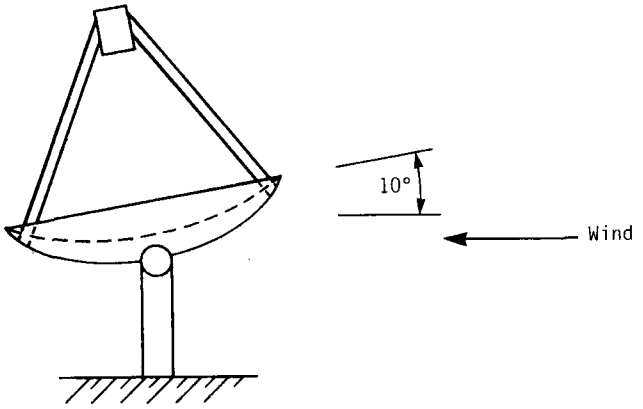

(a) Stowed, <10° Attack Angle, 90 mph Wind
(Maximum Lift and Elevation Moment)

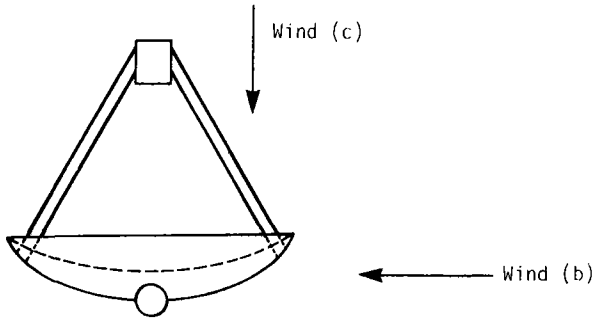

(b) & (c) Operating, Top View, Paraboloid Axis
Horizontal, 50 mph Wind
(b) Gives Maximum Azimuth Moment
(c) Gives Maximum Drag

Figure A.3 - Orientations of Dish for Maximum Wind Loads

The wind force coefficients used for troughs reflect both the worst-case combination of orientation and wind speed and the effect of the aspect ratio (length divided by width). The measured data on troughs (A-3) is primarily taken at an aspect ratio of 3.75 (i.e., length is 3.75 times aperture width), though sufficient data is presented to make adjustments to other aspect ratios. The design analyzed here has an aspect ratio of 12.5, and this results in increases of 26% for C_d, 58% for C_ℓ, and 81% for C_m, relative to the results for the 3.75 aspect ratio.

Specifications have been proposed for wind coefficients for use in trough design (A-9), as listed in Table A.2. These coefficients are intended to be used for calculating loads on a 3.75 aspect ratio trough in any orientation, assuming a wind fence of 25 to 35% porosity. The measured coefficients in upward-facing stow position, with or without a fence, are lower than the specified values. Even after increasing the coefficients for the 12.5 aspect ratio, the coefficients in stow position without a fence are less than the specified values, as shown by Table A.2. The specifications in (A-9) are too conservative, because they do not take into account the lower wind loads in stow position.

For dishes, the force and moment coefficients were calculated from radar antenna data presented in (A-10, A-11). The distance between the dish vertex and the elevation axis was assumed to be one foot for calculation of moment coefficients. These coefficients are somewhat less certain than the heliostat and trough coefficients, which are based in part on wind tunnel tests of actual collector models.

The design loads are calculated from Eqs. (A.1) through (A.3) and the coefficients tabulated in Tables A.1 through A.3. The necessary values of A, V, H and L for each collector are given in Table A.4. In calculating h, a ground clearance of one foot was assumed in all cases, and the offset between collector surface (vertex) and the elevation axis in stow position was one foot for the heliostat and dish, 0.5' for the trough. The trough is designed with $f/L = 0.25$ (90° rim angle), while the dish is designed with $f/L = 0.5$, where f and L are respectively the focal length and aperture distance (chord or diameter).

Table A.5 compares the calculated wind loads on the drive axes. In all cases, the wind forces on the backup structure are assumed to be included in the coefficients used. For heliostats, no additions for receiver, etc., are necessary. For troughs, the figures in Table A.5 include the additional drag of the receiver tube, which catches the wind in the face up position. This is considered a long tube with drag coefficient 1.2 and area 13.7 ft^2, resulting in an addition to 90 mph drag force of 200 lb. The lever arm is 2.2', so the addition to moment is 450 lb-ft.

TABLE A.4

WIND LOAD PARAMETERS

Technology	Gross Aperture Area A, ft^2	Chord L, ft	Survival (Leading Edge) Height h, ft	Survival (Leading Edge) Velocity V, ft/s	Operating (To Axis) Height h, ft	Operating (To Axis) Velocity V, ft/s
Parabolic Dish	541	26.2	20.7	125	14.1	65.5
Parabolic Trough	538	6.56	7.0	106	4.28	54.7
Heliostat	528	24.2 (elevation) 22.3 (azimuth)	16.2	120	13.1	64.7

NOTE: The height to the leading edge in survival stow position includes L/2 sin 10°.

TABLE A.5

WIND LOADS AT DRIVE AXES CORRESPONDING TO THE ORIENTATIONS IN FIGURES A.1 - A.3

Load Case	Dish Value	Dish Figure No.	Trough Value	Trough Figure No.	Heliostat Value	Heliostat Figure No.
Maximum Drag	3900 lb	A.3(c)	3800 lb	A.2(a)	3200 lb	A.1(b)
Maximum Lift	3800 lb	A.3(a)	3600 lb	A.2(a)	3800 lb	A.1(a)
Maximum Elevation Moment	43000 lb-ft	A.3(a)	13200 lb-ft	A.2(a)	24200 lb-ft	A.1(a)
Maximum Azimuth Moment	11700 lb-ft	A.3(a)	---		8800 lb-ft	A.1(c)
Additional Cases						
Stowed Drag	3500 lb	A.3(a)	---		1300 lb	A.1(a)
Negative Lift	---		3650 lb	A.2(b)	---	

For dishes, the figures in Table A.5 include the effect of the receiver and receiver struts. The receiver is assumed to be a cylinder, 2.15' diameter and 1.8' long, with drag coefficient 0.72. In stow position, it is 30' off the ground, so V = 132 ft/s and the additional drag force is 58 lb. This acts at a distance of 15.0' from the elevation axis, so the additional elevation moment is 870 lb-ft. At 50 mph, the receiver drag is 14 lb and the azimuth moment is 210 lb-ft. The three receiver struts are 3" schedule 40 pipe (OD = 3.5"), and approximately 13.2 ft of each is exposed above the rim of the dish. The riser and down-comer pipes and insulation are assumed to fit inside the support struts so that they do not add to the optical losses or the wind loads. Under these assumptions, 11.6 ft^2 of area is exposed, with drag coefficient 1.2 (long tube), and the average height of this area is 23.3' in stow position, 14.1' in operting position with dish axis horizontal. The receiver strut drag loads are 270 lb stow, 70 lb operating, and the moments are 2500 lb-ft elevation and 650 lb-ft azimuth.

It is apparent in Table A.5 that the lift and drag loads are similar for the three collectors, but the elevation moments are quite different. The elevation moment in stow position is considerably greater for the dish than the heliostat, because the drag force is greater (3500 vs. 3200 lb), and it acts at a greater distance from the axis. The trough moment is much less, because its chord is smaller (6.6' vs. 26') and it is closer to the ground, where the wind speeds are lower.

A.2.0 Design and Cost of Support Structures

In this section, the changes in heliostat structure are documented and the basic components of dish and trough structure are designed and costed. The dish and trough structures are designed to have the same stresses and deflections as the corresponding heliostat structure. Since the loads and configurations are different, so are total weights and the distributions of weight among main beams, hat sections, etc.

The basic source of cost data is the McDonnell Douglas Prototype Heliostat cost breakdown (A-13). The costs in (A-13) are in 1978 dollars; they have been increased by 10% to yield 1979 dollars. The costs for similar items in dishes and troughs (similar shape and function) are scaled to the same $/lb as for the heliostat. This procedure implicitly accounts for many minor design details that would not affect the cost comparison of the three designs (e.g., brackets, fasteners, stiffeners), while concentrating on the major differences that result from differences in loads and configurations. The accuracy of $/lb scaling is considered in Section 4.1.

A.2.1 Heliostat Structural Design and Cost

The structure of the heliostat is shown in Figure 3.1. The major difference from the design presented in detail in (A-13) is the elimination of the inverted stow capability. The main beam or "torque tube" is 24" shorter, reducing its cost and weight to $115 and 233 lb. The support beams (channel sections) are unchanged at 698 lb, $277, and the hat sections are unchanged at

336 lb, $161. All sections are assumed to provide an appropriate safety margin for the expected stresses and deflections as designed by McDonnell Douglas.

A.2.2 Dish Structural Design and Cost

The details of the dish structure are shown in Figure A.4. Analogous to the main beam or torque tube, there is a central hub 24" diameter by 22" long, 0.375" thick*, which weighs 200 lb. including all brackets, pivots, etc. Assuming the same $0.50/lb as the heliostat tube, this hub costs $100. Attached to the central hub are twelve (12) support beams, which are rolled channels as in the heliostat, curved along their length to define the radial parabolic shape.

Under worst-case wind loads, which occur in stow position, the beam that is aligned with the wind must withstand a moment equal to 1/3.73 times the elevation drive moment. In the heliostat, the two largest support beams each carry one-quarter (1/4) of the elevation moment. For equal stresses at the attachment to the main beam or hub, the relationship between the section properties and elevation drive moments is

$$\frac{Z_h}{Z_d} = \frac{M_h/4}{M_d/3.73} = 0.525 \qquad (A.5)$$

The section modulus for the heliostat beam is $Z_h = 9.32$ in^3, so the required modulus for the dish beam is $Z_d = 17.75$ in^3. For such a thin section (t = 0.0747" for the heliostat) a major problem is buckling. The AISC formulas specify

$$\frac{b_f}{2t} > 10.8 \qquad (A.6)$$

$$\frac{d_w}{t} > 107 \qquad (A.7)$$

where b_f is the flange width, d_w is the web height, and t is the material thickness. The MDAC design does not meet these guidelines, but if the dish beam is designed to be no more prone to buckling than the MDAC beam, the result is a channel section of 12 gage steel (0.1046" thick) that is 22" deep and has 4.19" flanges. This beam is slightly less prone to buckling than the heliostat beam, and it will have the same stresses in a 90 mph wind in stow position. The weight of the twelve curved beams in 1547 lb, and at the same $.40/lb as for the heliostat, the cost is $619. This is surely too low,

*Note: Diameter and length are determined by receiver shadow and support beam depth; thickness is estimated from shear strength at beam attachments. Detailed 3-dimensional analysis would be necessary for confidence in the chosen thickness. This uncertainty has negligible effect on total dish cost.

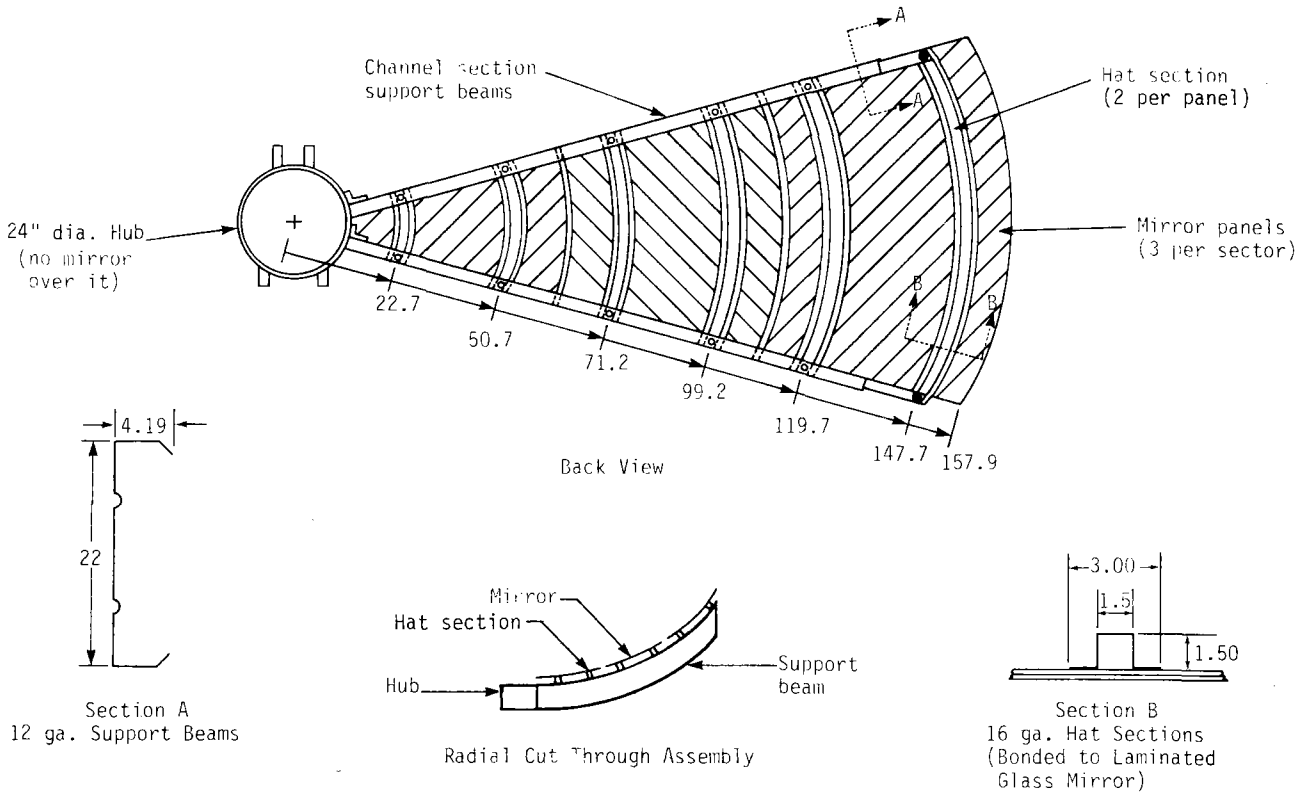

Figure A.4 - Details of Dish Structure (Dimensions in Inches)

because it generally costs more to manufacture a precise curve than to roll straight sections. As a more reasonable lower bound, assume that the curvature would add at least 5% to the cost, making it $650.

The deflection during a 30 mph (maximum steady operating) wind for the dish and heliostat beams was compared by considering both to be straight beams* with distributed loads that are proportional to mirror area. The dish beam has slightly less deflection in a 30 mph wind than the heliostat beam, but both angular deflections are less than 0.5 milliradian. Thus, there is no important performance difference.

The hat sections that are bonded to the glass are curved in one dimension as segments of a circle. As in the heliostat, the glass panels are nominally 4' wide, and the spacing between the two hat sections on each mirror panel is 28", as shown in Figure A.4. The greatest span for these hat sections, between support beams, occurs near the rim of the dish; it is 6.42', compared to 6.33' for the heliostat. The number of support beams was chosen to keep this span comparable so that the hat sections would not be overstressed. Each dish requires 286 lineal feet of hat sections, which weigh 370 lb, and at the same $0.47/lb as the heliostat hat sections, this would cost $175. However, the hat sections must be curved to a precise circle which can be bonded to a surface that is curved in two dimensions. Consequently, the cost should be higher than the straight heliostat hat sections, perhaps by 5%. Thus the hat sections cost $184 per dish.

The remaining structural part is the dish receiver support. This consists of three 3" pipes, schedule 40 (OD = 3.5", ID = 3.068"), each 197" long. Without detailed analysis, this is assumed to be an adequate design by comparison with the design in (A-10). The weight is 373 lb, and cost is estimated at $0.40/lb, leading to $149 for the receiver support.

A.2.3 Trough Structural Design and Cost

Support beams as used in the heliostat and dish are not needed for the trough, because the width of the trough is small by comparison. Sufficient structural support is provided by a main beam or torque tube running the length of the trough and hat sections supporting the width, as shown in Figure 3.3. The parabolic shape is maintained by bonding the hat sections, which are curved along their length, to laminated glass which has been curved to the proper shape. The glass area supported by a pair of hat sections is approximately 4' by 7.5'.

The hat sections are designed to have the same bending stress in the maximum moment condition as the heliostat support beam. This requires a section modulus of 0.5 in^3, which can be obtained from a 3" deep hat section, 14 gage (0.0747" thick). The worst-case operating deflection occurs in a 30 mph wind; it is the sum of maximum negative lift plus the dead load of 2035 lb of glass mirror. The calculated angular deflection, assuming a cantilever beam with uniform distributed load and neglecting the contribution of the glass, is less than 0.5 milliradian. The hat sections are rolled from a 9"

*Curvature can be neglected for $\rho/d > 10$, as is the case here (A-14).

wide strip, and 295 lineal feet are needed for each trough. The weight of this material is 674 lb, and at the same $0.47/lb as the heliostat hat sections, the cost would be $317. However, these hat sections are curved to a parabolic shape, which should add perhaps 5% to their cost, so the estimated cost is $333.

The main beam for the trough must withstand both bending and torsional loads with minimal deflections. The worst-case combination of bending loads occurs when the maximum negative lift is combined with the gravity load. To keep the deflection small and minimize the combined cost of support pedestals and the main beam, a three-point support is optimum. If the ratio of length of the longer spans to the shorter cantilever spans (see Figure 3.3) is 2.6, there will be equal deflections at the ends of the cantilevers and at the centers of the long spans. A beam that is circular in section, 11" diameter by 0.0474" thick (14 gage), will withstand the maximum operating load (30 mph wind) with less than 0.2" deflection and 2 milliradian slope error. The slope error is less than 1 milliradian everywhere except at the extreme ends of the trough. The maximum bending stress occurs in the 50 mph negative lift configuration; it is about 11000 psi.

Such a thin tube is prone to elastic buckling under torsional loading. To prevent elastic instability, the shear stress should be less than half of the critical value, given in (A-15) as

$$\tau' = \frac{E}{1-\nu^2}\left(\frac{t}{\ell}\right)^2 \quad 1.27\ \sqrt{9.64 + 0.466\ H^{1.5}} \tag{A.8}$$

where

$$H = \sqrt{1 - \nu^2}\left(\frac{\ell^2}{tr}\right) \tag{A.9}$$

E is the modulus of elasticity, ν is Poisson's ratio, ℓ the length (taken as 29.7', i.e., the longest span), and t and r are tube thickness and radius, respectively. For the present case, τ' = 1500 psi, and the shear in the tube at maximum wind moment is 5600 psi, about 45% of τ'. This is a barely adequate safety margin.

The angle of twist in the tube at maximum operating wind torque (30 mph, 45° elevation angle) is about 5 milliradians over the entire length of the tube. That is, if the trough were perfectly pointed at the sun in the middle, in a 30 mph wind both ends would have a pointing error of 5 milliradians. However, the maximum twist is less than half this for elevation angles greater than 60°, which corresponds to approximately 9:00 a.m. Considering the expected low incidence of operation during 30 mph winds, the short period of time each day and low insolation at the worst-case orientation, and the fact that the central third of the trough never experiences more than half the maximum twist, the energy loss from this degree of torsional flexibility appears to be acceptably small.

The 11" diameter, 14 gage tube is 984" long. Neglecting connections, it would weigh 700 lb, so with all connecting flanges, stub bars, fasteners, etc., the weight is estimated at 750 lb. At the same $0.50/lb as the heliostat main beam, the cost is $375.

The remaining trough structure is the receiver support. This is designed for a maximum deflection of 1 milliradian in the worst-case operating condition (parabola axis horizontal). The distance between supports is 8 ft (i.e., one support every other mirror panel), and for a 1" Schedule 40 pipe receiver, this leads to a 0.014" (0.7 milliradian) sag midway between supports, just due to the weight of the pipe plus fluid. Allowing an additional 0.3 milliradian sag for the struts, which are cantilever beams, the required moment of inertia of the supports is 0.337 in^4. A 2" square section, 14 gage (0.747" thick) will suffice, and for a 19.68" focal length, approximately 25" of material are required, including the connection to the main beam and the receiver tube. Thus, a total of 45 lb of steel is required, and at \$0.50/lb, the cost is \$22.

A.3.0 Design and Cost of Mirror Panels

The mirror panels for all three designs are made of laminated glass. The front sheet is 0.060" thick fusion glass, back-silvered and bonded to 3/16 inch float glass. The assembly weighs 3.38 lb/ft^2, so for the heliostat, the total mirror weight is 1785 lb. The cost is estimated as \$566 (A-13).

The mirror surface area for a parabolic dish is given by (A-16).

$$S = \frac{2\pi}{3}\left\{\sqrt{P(2x + P)^3}\right\} \qquad (A.10)$$

where $P = y^2/2x = 8$ for $f/D = 0.5$. This gives a ratio of glass surface area to aperture area of 1.06, neglecting all gaps. The total area is 573.6 ft^2. In fact, the area blocked by the receiver (3.6 ft^2) is not covered with glass, so the actual glass area is 570 ft^2. This area weighs 1927 lb, and at the same \$.32/lb (\$1.07/ft^2) as the heliostat, the cost would be \$612. This estimate is surely low, because the glass must be curved into a two-dimensional parabolic shape. Firm estimates of the cost of this process are not available, but it must cost at least 5% more than flat mirrors and perhaps as much as 50% more. At the minimum, the cost would be \$643.

The length of the parabolic cross section of the trough is given by (A-17).

$$S = \sqrt{4x^2 + y^2} + \frac{y^2}{2x} \ln\left[\frac{2x + \sqrt{4x^2 + y^2}}{y}\right] \qquad (A.11)$$

where $x = 0.5$ m, $y = 1$ m at $f/d = 0.25$. In this case, the ratio of surface area to aperture area is 1.15. Assuming there are 9 supports between the mirror panels, approximately 20" is lost from the mirror length, so for a 2' x 25' nominal size, the actual mirror surface consists of 20 panels 4' wide (24.4 m, or 3% less active area). Mirror area is 7.55' x 80' = 604 ft^2, which weighs 2041 lbs. Assuming a 5% cost increase for curving the glass, the cost is \$680.

A.4.0 Drive Sizing and Cost

The present heliostat drive is simpler than the one presented in (A-13), because of eliminating the inverted stow capability. There need not be a separate stow jack, nor a drag link to connect the two jacks. With these two changes, plus some rearrangement of the cost categories to include motors but exclude structural parts such as the main beam, the heliostat drive costs are $505 and $363 for the azimuth and elevation drives, respectively. The revised weights are 407 lb (azimuth) and 80 lb (elevation).

It is beyond the scope of this study to perform a detailed redesign of the heliostat drives for use with the dish and trough. Instead, scaling rules are used, based on typical variations of cost with output torque. The form of the scaling rule is

$$C(T') = C(T)\left(\frac{T'}{T}\right)^n \qquad (A.12)$$

where C(T) is the cost of a drive with torque T. Within any family of drives, such a scaling rule is a reasonably accurate means of predicting the increased cost of a higher capacity drive. Figure A.5 shows several cost vs. capacity curves, for various types of drives and for electric motors. The slope of these curves varies between n = 0.41 for hydraulic drives and n = 0.95 for double reduction helical gear boxes without motors. In the latter case, the effect of production rate is confounded with the effect of capacity, because the larger units are made in much lower quantity.

A typical exponent is n = 0.8, which corresponds to a commercial electric motor and gearbox combination (A-18). This exponent will be used for determining the costs of dish and trough drives. This is admittedly a crude approximation; it is evident in Figure A.5 that different designs follow different scaling rules. There also may be crossover points between drive types, where it is economical to switch to hydraulic drives above some torque level, for instance. This effect plus the availability of standardized motors, etc. implies that the true cost vs. output curve is a staircase-type function. However, a suitably broad range of exponents used in a sensitivity study can bound the effect of the power function approximation.

For the dish azimuth drive, the ratio of required dish and heliostat output torques is 1.33 = 11700/8800 (see Table A.5), so the cost increases by 26% to $634. For the dish elevation drive, the ratio of required output torques is 1.78 = 43000/24200, so the cost increases by 58% to $575. To determine shipping weight, assume the weights also scale as in Eq. (A.12), with n = 0.8, so the dish azimuth and elevation drives weigh 513 lb and 126 lb, respectively.

For the trough, with the 25 m axis oriented north-south, the drive must provide 180° rotation. Thus, the costs are scaled from the heliostat azimuth drive--not from the elevation jack which only provides about 90° rotation. The ratio of required trough and heliostat output torques is 1.50 = 13200/8800, so the cost increases 38% to $698. The weight, under the same scaling assumption, is 563 lb. If the trough were oriented east-west, a 90° range of

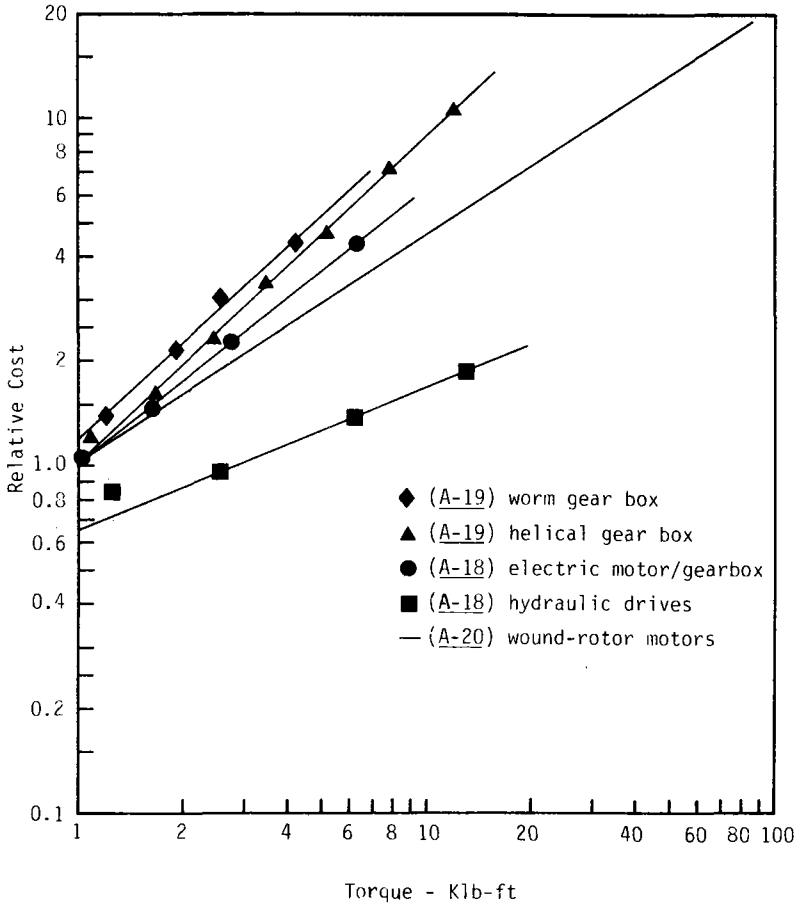

Figure A.5 - Relative Drive Cost vs. Output Torque

elevation tracking would work with minimal annual energy loss. The cost scaled from the heliostat elevation is $224, a savings of $474.

A.5.0 Pedestal/Foundation Design and Cost

The foundation considered here differs from previous work in several respects. The functions of pedestal and foundation are combined in a single precast, prestressed concrete pile. The pile is factory built at low cost and shipped to the field (500 miles assumed) where it is driven into place. It is hollow to minimize weight and driving forces, and it is fabricated with steel end plates for protection during driving and for easy attachment of the drives. Preliminary cost estimates indicate that such a pile would cost about two-thirds of the cost of the McDonnell Douglas field-poured foundation and steel pedestal.

For this study, prestressed pile designs are generated for all three technologies using consistent design rules. Prestress design is complicated, with several iterated analyses required. For this study, simplified design procedures were used to develop sufficient design detail for cost estimation. The designs have not been checked against all requirements of the Uniform Building Code, though certain code requirements are incorporated in the design rules described below. Except as noted,the approach is based on material in (A-21) and (A-22).

A.5.1 Design Approach

Most piles are designed as columns, to support a vertical load and possibly a modest side thrust. In this case, however, the vertical load (due to weight and negative lift) is negligible compared to the combined overturning moment of the drag force and elevation moment. For this reason, the basic design approach is to treat the pedestal as a cantilever beam, fixed 5' below grade. The primary design constraint is that bending stresses must be below the allowable values, which are 2250 psi compressive and 425 psi tensile for concrete with nominal 5000 psi ultimate strength. The estimated wind loads for this calculation are increased 27.5% from the values in Table A.5, as required by the Uniform Building Code.

Before the bending stresses can be calculated, several parameters in the prestress design must be determined. The final prestress in the concrete is taken to be 880 psi; in the steel tendons it is 160000 psi (for nominal 250000 psi ultimate strength tendons). The ratio of steel tendon area to gross section area is $A_s/A_g = 0.0055$, and the wall thickness of the hollow circular cylinder is fixed at 3 inches. This maintains at least 1" concrete cover over the reinforcing steel, which is acceptable under the precast concrete building code rules.

The pedestal diameter is determined by setting the bending stress on the compression side equal to approximately 2250 - 880 = 1370 psi. The maximum tensile stress is similarly calculated as approximately 1370 - 880 = 490 psi. In fact, both compressive and tensile stresses are modified slightly by the

compressive stress arising from the weight of the concentrator minus lift forces, and this is considered in the design. The tensile forces are actually carried by the steel tendons, but the calculated stress in the concrete must not exceed the allowable 425 psi or cracking might occur. The change in tendon stresses due to bending is a small fraction (typically 5%) of the prestress value.

The required depth for the pile is given by

$$d^2 = 0.00878 \frac{P}{b} \left(1 + \sqrt{1 + 248.4\ hdb/P}\right) \qquad (A.13)$$

where d is the depth, b is the outside pile diameter, and P is an equivalent lateral load acting at height h above the ground. The value of P is calculated by

$$P = (F_d \cdot h_a + M_e)/h \qquad (A.14)$$

where F_d is the drag force at the drive axis (height h_a above the ground) and M_e is the elevation moment. Eq. (A.13) is based on empirical data and simplifying assumptions regarding the distribution of soil resistance, as discussed by (A-23). The numerical constants incorporate the bearing strength of the soil, taken here as 133 lb/ft^2 per foot of depth for mixed sand and gravel (A-24). The deflection under operating winds can be calculated once the depth is known, using a standard cantilever formula for the portion above grade and

$$\delta = 18P\ (1 + 1.33h/d)/(42000d^2) \qquad (A.15)$$

for the portion below grade (A-24). The total deflection is approximately 1 milliradian for the designs presented here.

The total length of the pile is approximately $d + h_a - 2$, where the assumed height of the drive is 2 ft. The volume of steel tendons and concrete can then be estimated from their respective areas, and their material costs are \$.50/lb and \$52/yd^3, respectively. An empirical relation for the required volume of the spiral steel wrapped around the tendons is

$$V = 0.0375\ (A_g - A_c)\ \ell \qquad (A.16)$$

where $A_g - A_c$ is the area of the annulus between the outer surface of the pile and an imaginary circle enclosing the steel tendons, and ℓ is the pedestal length. The spiral steel material cost is estimated at \$.40/lb, as is the cost of the end caps.

The cost estimate is built up from labor and materials estimates, using the material costs noted above plus selected detailed costs from (A-13), increased 10% to 1979 dollars. Shipping cost for the completed pile is based on 500 miles shipping at \$6 x 10^{-5} per pound per mile. The cost of driving the pile in place is estimated from time estimate data supplied by ABAM Corporation (A-25); the major cost is setup and moving between locations. As a function of pile depth, the cost is

$$\text{Driving Cost} = \$1.17d + \$53 \qquad \text{(A.17)}$$

The production scenario includes a factory with prestress beds, production tooling including molds and cores, cutoff and materials handling equipment, and a dedicated concrete plant. The amount of factory labor is small and independent of pedestal size.

A.5.2 Results of Design and Cost Estimates

The final pedestal dimensions and costs are presented in Table A.6 for all three technologies. The greater wind moments on the dish and heliostat are carried by increasing the diameter of the piling as necessary to maintain the same stress. The depth below grade also increases, but not as dramatically. The depths are of course only valid for a particular soil, in this case mixed sand and gravel that will laterally support 133 lb/ft^2 per foot of depth.

Combining two side pedestals and a center pedestal, the cost of trough pedestals is $746, highest of the three technologies. The reason is the need for three separate pedestals to support the long trough. The costs of surveying, driving the pile, and pouring and separating piles in the factory do not vary much with pile size. Raw material and shipping costs do vary with size, but the structural efficiency of small pedestals is lower, so that these costs are about the same for three small pedestals as for one larger one that carries twice the total load. The mechanical attachment costs, including bearings on the side posts, are higher for the trough, as well.

A.5.3 A Pedestal Cost Scaling Rule

The four pedestal designs given in Table A.6 correspond to completely different wind loading situations. However, the designs can be compared on a unified basis by expressing all loads in terms of the pedestal bending moment 5 feet below grade, assuming that the pedestal is a cantilever beam fixed at that point. For this comparison, the loadings in Table A.5 (not increased 27.5%) are used.

On log paper, the relationship between installed pedestal cost and bending moment is linear, as shown in Figure A.6. The corresponding functional form is

$$\text{cost} = 63.1\ (\text{Moment})^{1/2} \qquad \text{(A.18)}$$

where cost is in 1979 dollars and moment is in thousands of lb.-ft. (i.e., kip ft.). This is a good fit, with correlation coefficient $R^2 = 0.99$, and it is very convenient for cost estimation without redesign.

TABLE A.6

PEDESTAL/FOUNDATION DESIGNS AND COSTS
ONE-PIECE PRESTRESSED HOLLOW CONCRETE PILE

	Dish	Trough		Heliostat
		Center	Side*	
Outside dia, in.	28.5	15.5	11.5	21.5
Inside dia, in.	22.5	9.5	5.5	15.5
Tendon area, in^2	1.32	0.65	0.44	0.96
Spiral steel, in^3	1367	346	219	883
Total Length, ft	23.9	11.6	10.3	20.8
Length Below Grade, ft	11.9	8.4	7.0	10.0
Concrete Weight, lb	5600	1335	803	3550
Steel Weight, lb	560	157	101	368
Shipping Weight, lb	6260	1540	950	4000
Raw Material, $	311	83	52	202
Field Labor $	98	94	93	96
Factor Labor, $	33	33	33	33
Fasteners, Electrical Box, Miscellaneous, $	47	47	15	47
Shipping, $	188	46	29	120
Total Cost, $	677	302	222	498

*Two side pedestals per trough required.

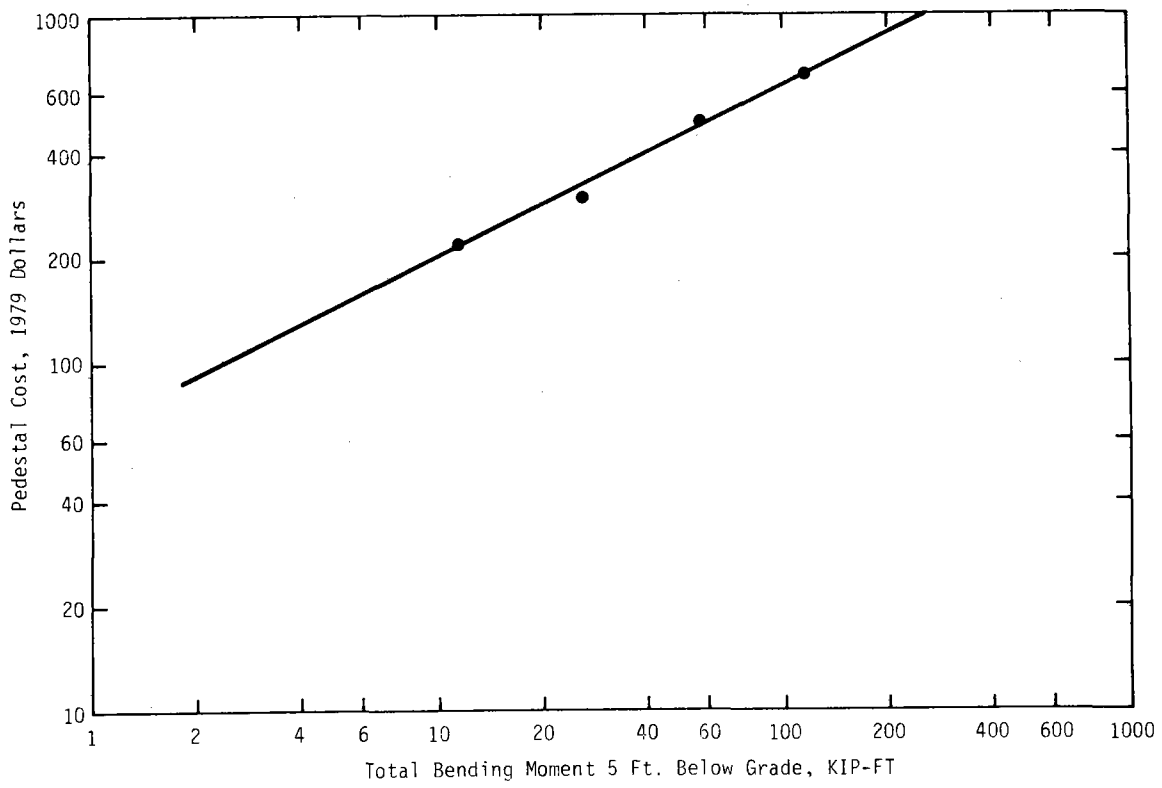

Figure A.6 - Installed Pedestal Cost vs. Bending Moment Due to Maximum Wind Loads. Cost Includes Factory Materials and Labor, Shipping and Installation for Prestressed Concrete Piles.

A.6.0 Other Cost Elements

There are several cost items not included in the major categories above. In some cases, the differences between technologies imply differences in the costs, and the assumptions made are described in detail here.

Controls and wiring for the new heliostat are identical to the design presented in (A-13). Adjusted to 1979 dollars, the cost of this subsystem is $381. However, for dishes, the control system is much simpler. Except for removal from service for maintenance, all dishes in the field track the sun together. Approximately $135 out of the $381 for heliostats is devoted to the microprocessor on each heliostat plus a proportionate share of the central computer. Assume that this cost is cut by $72 and redistributed, with most tasks covered by the central computer. Then the dish control/wiring cost is $309, assuming all other aspects are the same as heliostats.

The same reduction in control costs applies to the troughs (-$72), but in addition there is only one motor to control. Thus, the motor controller is half as expensive (-$18), and the cost of wire, transformers, etc., is similarly cut (-$79). The net effect of these changes is a reduction to $213 for the control and wiring category. What is left is basically a local motor controller, field and local wiring for one motor per trough, wiring installation, and central control. Note that open loop direct digital control with occasional calibration is assumed for all three technologies.

Installation of the drives on the pedestal and the mirror panels on the drives follows the scenario presented in (A-13) for heliostats and dishes. The drives are pre-assembled and checked out, ready to bolt in place and connect cables to the factory-wired electrical boxes. The mirror panels are shipped in two large assemblies, factory aligned and jig-drilled to bolt to the drives. Special field handling equipment permits rapid attachment with small crews, and sun acquisition and tracking calibration is semi-automatically conducted under computer control when installation is complete.

The installation cost for the dish is expected to be somewhat greater than for the heliostat, because the two major mirror assemblies must be field-connected along two of the radial beams. This means six mirror panels must be connected in the field, where in the heliostat scenario, the only field connection is structure to drive. This extra step is estimated at two (2) man-hours (if suitable jigs are designed), so it results in an extra cost of $56 for the dish. Additional time, perhaps two man-hours ($56), will be required to connect the receiver and support struts to the dish structure.

The installation of the trough is considerably complicated by the need to ship and align the two outboard bearings with the drive. In addition, the trough panels would be shipped in four pieces, requiring twice as many connections as the heliostat. The extra time required is estimated at 5.4 man-hours ($151). The receiver struts are assumed to be factory installed, and the cost of receiver installation is included with receiver costs.

An additional cost difference arises from weight differences in shipping from factory to site for the structure, mirror, and drives (recall that the pedestal shipping cost is included in the pedestal/foundation cost category).

The weights of these items and associated shipping costs for 500 mi at \$6 x 10^{-5}/mile/lb are shown in Table A.7. The major differences in weight arise from differences in glass surface area and steel structure. An assumed weight differential for packaging the unattached dish mirror panels and the trough sections adds \$6 and \$3 respectively to the dish and trough shipping costs.

TABLE A.7

ESTIMATED SHIPPING WEIGHT AND COST FOR 500 MILES EXCLUDING PEDESTALS

	Dish	Trough	Heliostat
Mirror Weight, lb	1927	2041	1785
Structure Weight, lb	2067	1424	1267
Drive Weight, lb	639	563	487
Number of Assemblies	9	5	3
Estimated Expendable Packaging Weight, lb	300	200	100
Shipping Weight, lb	4933	4228	3639
Shipping Cost, \$	148	127	109

All other cost components are the same for the three technologies. This includes such items as calibration, checkout, field maintenance equipment and spare parts. Including installation amd shipping plus these constant costs, the "Installation and Other" costs for dishes, troughs, and heliostats are \$453, \$527, and \$358, respectively.

APPENDIX B--DETAILS OF SENSITIVITY STUDIES

B.1.0 Sensitivity of Dish Cost to Size

As dish diameter increases, mirror area increases as D^2. However, the wind induced moments, which govern the design of structure, drives, and pedestal, increase as $D^{3.3}$. This is evident by inspection of the wind moment equation (A.3), where V is given by Eq. (A.1). Combining all constants,

$$M = 0.881\ D^3\ h^{0.3} \tag{B.1}$$

and h is roughly proportional to D. To maintain equal stresses (M/Z), the section modulus Z must also increase as $D^{3.3}$.

The radial support beams act as cantilever beams, with distributed loading that increases with distance from the hub because the mirror area for each beam is wedge shaped. For a linearly increasing distributed load, the angular deflection at the tip of a cantilever of length ℓ is

$$\theta = \frac{w_{max}\ \ell^3}{8EI} \tag{B.2}$$

The length of the beam depends on dish diameter, and so does the maximum load w_{max}. Consequently, angular deflection is proportional to D^4, and can only be held constant by increasing the moment of inertia I proportional to D^4. Since $Z = I/c$, the goals of equal-stress design and equal-angular-deflection design are equivalent for linearly increasing radial load and beam depth 2c that is proportional to $D^{0.7}$.

For support beam design, the equal-stress approach is taken; that is, section modulus Z is scaled up by $D^{3.3}$, and empirical relationships are used to determine the appropriate cross section area, A, and beam depth, h

$$A = 0.460Z^{0.656} \tag{B.3}$$

$$h = 8.476Z^{0.345} \tag{B.4}$$

These formulas are curve-fits to 5 lightweight channel-section beam designs over the range $18.75 \leq h \leq 48$, using the design approach in Appendix A to

ensure comparable margin against buckling. The fits are excellent, with correlation coefficient $R^2 = 0.99$. If $Z = I/c$ increases as $D^{3.3}$ and $h = 2c$ is given by (B.4), I increases as $D^{4.4}$, and the approach taken here results in equal stresses and slightly decreasing angular deflections as dish diameter increases.

Twelve support beams are used in all cases, so the length of glass between beams at the rim of the dish increases as diameter increases. Consequently, the hat sections for the outer glass panels must be made stiffer as diameter increases in order to avoid unacceptable sag between support beams. The criteria used for design are:

(a) Use the heliostat hat section design for all panels out to 8 m diameter.

(b) Design stiffer hat sections for the panels beyond 8 m diameter by matching the maximum angular deflection at the furthest-out hat section of the 8 m dish and the larger design. The scaling is $I \sim (\ell/6.446\ \text{ft})^3 m$ where ℓ is the arc length between support beams for the furthest-out hat section. To derive this rule, the hat sections are assumed to be simply supported beams, loaded along their length with a uniform load per unit circumference that is independent of radius.

(c) For smaller diameters, design less-stiff hat sections using the same approach as (b).

The central hub is designed by geometric scaling only. The length is equal to the beam depth and the outer diameter is equal to the diameter blocked by the receiver. The receiver aperture diameter scales as dish diameter for equal concentration ratios, but the thickness of insulation is constant, so hub diameter does not vary exactly with dish diameter. The thickness of the hub is scaled to hub diameter. This is a crude scaling approach to a fairly complex, three-dimensional loading situation. In fact, the hub design would probably deviate from the simple pipe section as diameter increases, but it is reasonable to expect the amount of material to vary approximately as D^3, as it does with the above approach, because the wind moment that must be carried through the hub varies as $D^{3.3}$.

In addition to the wind moment on the dish, the drives must carry the moments caused by drag on the receiver and receiver supports in stow position. The diameter and length of the receiver vary with dish diameter (taking into account the constant insulation thickness), and for constant f/D ratio, the moment arm about the drives also varies with diameter. The receiver struts are used in tension and compression, not bending, so their cross-section area must vary with receiver weight or wind drag (D^2 in either case). The moment arm, which is the distance between the center of pressure and the drive axis, is also proportional to D. Combining all effects, the total elevation and azimuth drive moments vary approximately as $D^{3.3}$. The drive costs and weights are scaled from this required output torque as in Section A.4.0.

The pedestal cost is determined from the bending moment 5' below grade, as described in Section A.5.3. For this calculation, the drive moments determined above are combined with the moments of the drag forces on dish

and pedestal. These moments are also proportional to $D^{3.3}$, and combined with the cost scaling law which depends on $(\text{moment})^{1/2}$, the pedestal cost increases more slowly than the aperture area, as $D^{1.6}$.

Many of the control and wiring costs are constant, but the cost of wiring and wiring installation is affected by the current draw of the drive motors. Current appears to be proportional to motor power or torque raised to the 0.8 power (B-1), and the cost of electrical cable is assumed to be proportional to current capacity raised to the 0.8 power. Hence, the cost of wire is proportional to $(\text{torque})^{0.64}$ and torque is directly proportional to moment, which varies as $D^{3.3}$. There is a constant cost of \$101, and the balance, \$208, is assumed to vary as $(D^{3.3})^{0.64} = D^{2.1}$. The overall effect of the large constant cost is that the Control and Wiring category increases more slowly than area, at least for sizes up to 200 m^2. The same result is noted in the Installation and Other category, where a large constant cost partially compensates for shipping costs that increase with weight (roughly D^3) and installation costs that are assumed to increase with aperture area for the larger dishes.

The cost breakdown as a function of size is given in Table B.1. The categories Drives and Structure are responsible for the diseconomy of scale; all other categories show proportional costs or an economy of scale. For reference, the cost of the receiver struts, including material and installation, is also given.

B.2.0 Sensitivity of Trough Cost to Size

B.2.1 Longer Troughs

The trough described in Appendix A is 25 m long in order to have roughly the same aperture area as the heliostat and dish. However, this is not necessarily the optimum length for troughs. As the length of the trough increases, drives, controls, and wiring costs per unit area decrease. The costs of glass and hat sections stay constant (per unit area), but the cost of the main beam increases because it must become torsionally stiffer as it gets longer to maintain the same maximum twist angle. Increased torsional stiffness also provides increased bending stiffness, so the pedestals can be spaced further apart to reduce the pedestal cost per unit area. The interaction of the various component cost increases and decreases can cause either overall cost increases or decreases.

The main beam is sized primarily for equal deflections. The first step is to determine diameter and thickness such that the worst-case angle of twist from trough end to drive is constant (4.8 milliradians). The ratio of thickness to diameter is held at about 0.005 to maintain some margin against elastic instability (which is checked using Eq. (A.8), (A.9) once the length between supports is known). The diameter and thickness determine the bending stiffness as well, and the support spacing is determined from the requirements that worst-case angular deflection must not exceed 1.8 milliradians and deflection must be equal in the supported and cantilever sections (see Figure 3.3). The number of required supports is an odd integer for a symmetric design.

TABLE B.1

COST BREAKDOWN FOR DISHES OF VARYING SIZES
1979 DOLLARS

	Active Aperture Area			
	22.4 m^2	49.3 m^2	86.9 m^2	197.6 m^2
Mirror Surface	$ 295	$ 643	$1,134	$ 2,590
Drives	450	1,209	2,484	7,407
Controls and Wiring	196	309	480	987
Structure: Hat Sections	37	184	346	1,104
Support Beams	162	650	1,467	5,839
Hub	22	100	244	600
Pedestal/Foundation	393	677	1,028	1,924
Installation and Other	360	453	641	1,361
Total $/Unit	$1,915	$4,225	$7,824	$21,812
Total $/$m^2$ Aperture	$85/$m^2$	$86/$m^2$	$90/$m^2$	$110/$m^2$
Receiver Struts	$5/$m^2$	$4/$m^2$	$4/$m^2$	$4/$m^2$

Note: Costing assumptions are as noted on Table 3.3 All costs are scaled from the baseline 49.3 m^2 design using simplified redesign rules.

The pedestal costs are determined from the scaling rule, Eq. (A.16). The total moment on the center pedestal 5' below grade is the sum of the drive moment, which is proportional to trough length, and the moments arising from drag forces, which are also proportional to length. For simplicity, each of the n pedestals is assumed to carry (1/n)th of the drag load. The side pedestals are designed for drag-induced moments only.

The wiring costs increase for longer troughs, depending on the current requirements of the drive motors. The same procedure as in Section B.1 is used, but here torque is proportional to length (or equivalently, aperture area). Installation of the cables is assumed constant at $57 for trough lengths up to 25 m, then proportional to (trough length)$^{0.64}$ to account for the greater difficulties of handling the larger cables. All other control and wiring costs ($83) are independent of trough length. The overall effect is reduced control and wiring costs per unit aperture as trough length increases.

The drive is sized for the wind moment, according to Eq. (A.12). Mirror surface and hat section costs are proportional to aperture area or trough length. Shipping cost is proportional to weight, excluding the pedestals because their shipping costs are implicitly included in Eq. (A.16). Alignment cost related to the multiple pedestals is assumed to be proportional to the number of pedestals, and all other calibration and checkout costs are independent of trough length.

Table B.2 shows the results of these calculations. The primary effects are proportional costs for mirror surface and hat sections, a diseconomy of scale for the main beam, and economies of scale for all other components. The unfavorable scaling of the main beam cost arises from the fact that the angle of twist is proportional to the trough length squared, so maintaining the same twist angle as length doubles requires four times the torsional stiffness (which results in a beam that is approximately 3 times the weight and cost).

Note that the simplified redesign rules used here do not reflect possible design concept changes that might reduce the costs. For example, the main beam in the 200 m trough is approximately 31 inches in diameter and 0.21 inches thick. It is unlikely that the beam and hat section concept would be maintained to such an extreme; a monocoque or semi-monocoque structure of equivalent torsional stiffness would probably be used instead. Determining the crossover point for such design concept changes is outside the scope of this work.

B.2.2 Wider Troughs

The effect of wider troughs is considered by generating a point estimate of the cost of a trough that is twice as wide. The wind moment is proportional to $(\text{width})^{2.3}$, analogous to Eq. (B.1) for dishes. Thus, twice the width implies 4.92 times the moment, and the hat sections must be replaced by beams with 4.92 times the section modulus to maintain equal stresses and comparable deflections. The scaling rules given by Eq. (B.3) and (B.4) are used to determine the area and depth of the required beams, with the result that area, weight, and cost increase to 2.46 times the baseline hat section values, i.e., \$819 and 1657 lb.

The twisting moment on the main beam also increases as $(\text{width})^{2.3}$, and the primary constraint is found to be elastic stability. The methods described in Section A.2.3 are used to determine that the appropriate section is 16" diameter, 0.125" thick. The cost and weight are 2.42 times that of the baseline trough, i.e., \$906 and 1812 lb.

To check the bending load on the beam, a revised estimate of worst-case loading was generated. The glass mirror weight per unit length doubles, so that a 25 m trough carries 4082 lb of mirrors, costing \$1362. The negative lift load also increases, according to $(\text{width})^{1.3}$, following the same reasoning as for Eq. (B.1). Considering the increased structural weight, glass weight, and negative lift, the unit loading is 17 lb/in, 2.3 times that of the baseline trough. The resulting stresses and deflections are acceptably low (7 ksi, 1 milliradian).

TABLE B.2

COST BREAKDOWN FOR 2 m WIDE TROUGHS OF VARYING LENGTH, 1979 DOLLARS

	Trough Length				
	7.4 m	25 m (Baseline)	50 m	75 m	200 m
Mirror Surface	$ 204	$ 680	$1,360	$ 2,040	$ 5,440
Drives	264	698	1,215	1,682	3,685
Controls and Wiring	170	213	286	346	575
Structure: Hat Sections	100	333	666	999	2,664
Main Beam	111	375	1,344	2,925	23,880
Pedestal/Foundation	240	746	1,298	1,655	3,185
(Number)	(1)	(3)	(5)	(5)	(7)
Installation and Other	290	527	777	902	2,830
Total $/Unit	$1,379	$3,572	$6,946	$10,549	$42,259
Total $/$m^2$ Aperture	$97/m^2$	$75/m^2$	$73/m^2$	$74/m^2$	$111/m^2$

Note: Costing assumptions are as noted on Table 3.3. All costs are scaled from the Baseline (North-South) result, using simplified redesign rules. For East-West troughs, multiply drive cost by 0.321; all other costs are unchanged.

Drive cost scales as $(\text{width})^{1.84}$, and since area is proportional to width, there is a diseconomy in this cost category. The estimated cost and weight are \$2500 and 2015 lb. Controls and wiring are scaled as in Section B.2.1, leading to a cost of \$353. Installation and Other is the same as the baseline value, except for increased shipping cost and an assumed extra manhour for handling the larger sections. The total is \$726 in that category. The pedestal design relies on the scaling rule of Section A.5.3, with drag loads that vary as $(\text{width})^{1.3}$ and moment that is 4.92 times the baseline value. The side pedestals each cost \$399 and the center pedestal costs \$647, for a total pedestal/foundation cost of \$1445.

The sum of the cost categories is \$8111 for a trough with twice the active aperture area (i.e., 95 m^2). Thus, the cost is \$85/m^2, 13% higher than the cost of the baseline design and 16% higher than the cost of an equal-aperture trough that is twice as long. It appears that the optimum way to add area to a trough is by increasing length, not width. The principal reason is that the loads vary with length to the first power, but with width to the 1.3 or 2.3 power.

B.3.0 Sensitivity of Trough Cost to Structural Stiffness

The concentration ratio (concentrator aperture/receiver aperture area) is lower for troughs than for dishes or heliostat fields. This means that the receiver is relatively larger and easier to hit, or equivalently, that structural errors resulting in imperfect focus are less important. A reasonable question is how much cheaper could the trough be if it were designed for greater maximum structural deflections?

The baseline design developed in Appendix A was designed for deflections comparable to heliostat deflections. It is a deflection-constrained design in several components: main beam (torsional and bending), number of pedestals (bending of main beam), and hat sections (bending). A stress limited variant of this design with greater deflections is developed here.

The first issue addressed is the minimum number of pedestals. A single pedestal would work for 50 m^2 aperture, but the resulting main beam cost increase exceeds the pedestal cost decrease. The configuration that optimizes the tradeoff between main beam and pedestal costs for 50 m^2 is two pedestals, which results in an asymmetrically-placed drive. With an 8" OD main tube, 14 ga (0.0747" thick), the maximum angular deflections and stresses are acceptable in the two cantilever sections, (0.026 rad. and 43 ksi, respectively). This cross-section is unacceptable for the center span, however, because it has no margin against buckling, as determined by Eq. (A.8) and (A.9). A 12 gage beam (0.1046" thick) does provide adequate margin for buckling, and the resulting deflection is 3" in the center of the 559" span, with 36 ksi maximum stress. The twist angle in worst case operation (45°, 30 mph wind) is 0.014 rad. The resulting variable-section beam is 9% lighter than the baseline beam, and the deflections are 3-10 times larger.

In Appendix A, the hat sections were made deeper and thicker to yield stresses and deflections similar to the heliostat main beams. If the original

heliostat hat sections are used instead, i.e., 1.5" deep, 3" wide and 0.0635" thick, the maximum bending stress is 15 ksi and the maximum angular error is 0.00368 rad. This is about 4 times the heliostat deflection and 10 times the deflection of the baseline trough hat sections. The resulting hat section weight and cost is only about 57% of the baseline design weight.

The cost of the two pedestals is lower by 17%, even though together they withstand the same moment and drag as the three baseline pedestals. This is because larger pedestals are structurally more efficient, and because the constant per pedestal costs of surveying, moving between locations, etc. are reduced by one-third. The pedestal design procedure described in Section A.5.1 is stress-limited with negligible deflection, so there is no trade-off between cost and deflection to exploit.

Other costs that are affected by the redesign are alignment (down by $101 because of two pedestals instead of three) and shipping (down $11 because of 358 lb. weight reduction). All other costs are unchanged, including mirrors, drives controls and wiring, and calibration, checkout, etc.

Other costs that are affected by the redesign are alignment (down by $101 because of two pedestals instead of three) and shipping (down $11 because of 358 lb. weight reduction). All other costs are unchanged, including mirrors, drives, controls and wiring, and calibration, checkout, etc.

The overall effect is a cost reduction of $412 for north-south troughs, to $66/$m^2$ (active aperture). Thus, a trough with 3-10 times greater worst-case structural deflections could be about 12% cheaper. East-west trough designs show the same 12% reduction, to $56/$m^2$ (active aperture).

A slightly greater cost savings is obtained if an extra pedestal and a second 46.6 ft. section is added to the two pedestal design. This results in a symmetric three-pedestal design, as shown in Fig. 3.3, with the same maximum deflections and stresses as calculated for the two-pedestal design. The drives and pedestals are the only components that must be redesigned.

The three-pedestal trough is 39 m long, has an active aperture area of 74.4 m^2, and costs $63/$m^2$ for a north-south trough. Thus, the combination of greater structural error with a longer trough can yield costs that are slightly (~ 4%) lower than heliostat costs. The greater flexibility will result in a reduction in annual energy collection of unknown magnitude, so it is not obvious that this change is cost effective.

B.4.0 Effect of Variation in Wind Coefficients

The effect of variation in the wind force and moment coefficients is estimated here for each affected cost category. As shown by Eq. (A.2) and (A.3), errors in the wind coefficients cause equal errors in the calculated forces and moments. The purpose of this section is to trace the effects of assumed errors to determine their effect on total concentrator costs.

The primary design load on the dish structure is the wind moment. For the support beams, a 25% increase in moment requires a 25% increase in section modulus to maintain equal stresses and comparable deflections (see Sections B.1 and A.2.2). This, in turn, requires an increase in beam area and cost according to Eq. (B.3); for a 25% variation in moment coefficient, the beam cost increases 15.8%. The effect on hub cost cannot be easily calculated, because of loading complexity, but it can be ignored because hub cost has negligible leverage on total cost.

The hat sections are similarly affected by moment variations. Based on four individual hat section designs, an appropriate scaling rule for hat section area is

$$A = 0.831\ (Z)^{0.442} \tag{B.5}$$

This is a good fit ($R^2 = 0.998$) over the range $0.168 \leq Z \leq 0.661$ in^3. A 25% variation in Z produces a 10.4% variation in hat section area and cost.

The effect on drive scaling is given directly by Eq. (A.12) with n = 0.8. For a 25% change in all wind coefficients, moment due to receiver and strut drag will vary by 25%, as will moment on the dish itself. The effect of drive cost is a 19.5% variation in cost. Similar reasoning for the pedestal, using Eq. A.18, leads to 11.8% variation in cost.

The effect on total cost of a 25% variation in wind coefficients is the sum of the component effects above. Referring to Table B.1, the change in cost is

$$\Delta\$ = 0.158(650) + 0.104(184) + 0.195(1209) + 0.118(677) = \$437 \tag{B.6}$$

This is 10.4% of the total dish cost.

For troughs, the same reasoning leads to the same 10.4% variation in hat section cost, a 19.5% variation in drive cost, and 11.8% variation in pedestal cost. To estimate the effect of coefficient variations on main beam cost, an equation was developed from the baseline and double-wide trough beam designs. The independent variable is torque, because the limiting constraints appear to be twist angle and torsional buckling. The same power function form is used, resulting in

$$A = 2.21\ (T)^{0.55} \tag{B.7}$$

This is an exact fit to the two point designs. A 25% variation in coefficients results in a 25% torque variation, which in turn causes a 13.1% variation in cross-section area and cost. Referring to Table B.2, the effect on total cost is given by

$$\Delta\$ = 0.131(375) + 0.104(333) + 0.195(698) + 0.118(746) = \$308 \tag{B.8}$$

This is 8.6% of the total baseline trough cost.

It is important to note that at different dish and trough size, the cost categories have different relative magnitudes. Hence, the overall sensitivities will change with concentrator size.

REFERENCES

1-1 Solar Thermal Conversion Mission Analysis - Southwestern United States; Aerospace Corporation; ATR-74(7417-16)-1; November, 1974.

1-2 Solar Thermal Electric Power Systems; Colorado State University; PB243835; November, 1974.

1-3 Comparative Ranking of 0.1-10 MW_e Solar Thermal Electric Power Systems; Solar Energy Research Institute; SERI/TR-351-461; August, 1980.

1-4 Assessment of Solar Options for Small Power Systems Applications; Pacific Northwest Laboratory; PNL-4000; September, 1979.

1-5 Techno-Economic Projections for Advanced Small Solar-Thermal Electric Power Plants to Years 1990-2000; T. Fujita, et al.; Jet Propulsion Laboratory, JPL79-25; November, 1978.

1-6 Design, Cost and Performance Comparisons of Several Solar Thermal Systems for Process Heat; Volume I: Executive Summary; P. J. Eicker, et al.; Sandia National Laboratories, SAND79-8279; March 1981.

1-7 Design, Cost and Performance Comparisons of Several Solar Thermal Systems for Process Heat; Volume III: Receivers; James B. Woodard; Sandia National Laboratories, SAND79-8281; March, 1981.

1-8 Design, Cost and Performance Comparisons of Several Solar Thermal Systems for Process Heat; Volume IV: Energy Centralization; J. J. Iannucci and L. D. Hostetler; Sandia National Laboratories, SAND79-8282; March, 1981.

1-9 Design, Cost and Performance Comparisons of Several Solar Thermal Systems for Process Heat; Volume V: Systems; P. J. Eicker, J. D. Hankins, L. D. Hostetler, J. J. Iannucci and J. B. Woodard, Sandia National Laboratories, SAND79-8283; March, 1981.

2-1 Blackmon, J. B., "Non-Inverting Heliostat Study," Interim Report on Contract No. AD/03/01, McDonnell Douglas Astronautics Co., March 1979.

2-2 Easton, C. R., "Solar Central Receiver Prototype Heliostat CDRL Item B.d," McDonnell Douglas Astronautics Co., Report No. MDC G7399, August 1978, Volume II, Appendix H Detailed Cost Work Sheets.

3-1 Easton, op. cit., Section 2.3.

3-2 Eason, E. D., "The Credibility of Cost Estimates for Mass-Produced Heliostats," Sandia Laboratories Report SAND79-8222, October 1979.

3-3 Drumheller, K., et al., "Heliostat Manufacturing Cost Analysis: Vol. I," Solar Energy Research Institute Report TR-8043-1, October 1979.

3-4 Britt, J. F., et al., "Heliostat Production Evaluation and Cost Analysis," Solar Energy Research Institute Report TR-8052-1, December 1979.

4-1 Bergeron, K. D. et al., "Line-Focus Solar Thermal Energy Technology Development, FY79 Annual Report for Department 4720," Sandia Laboratories Report SAND80-0865, April 1980.

4-2 Shaner, W. W. and Wilson, H. S., "Cost of Paraboloidal Collectors for Solar to Thermal Electric Conversion," Solar Energy, Vol. 17, 1975, pp. 351-358.

4-3 Fish, M. J. and Dellin, T. A., "Heliostat Design Cost/Performance Trade-offs," Sandia Laboratories Report SAND79-8248, November 1979.

4-4 Truscello, V. C., letter to G. Braun, August 14, 1979.

4-5 Tallerico, L. N., "A Description and Assessment of Large Solar Power Systems Technology," Sandia Laboratories Report SAND79-8015, August 1979, p. 49.

4-6 Eason, E. D., "The Cost and Value of Washing Heliostats," Sandia Laboratories Report SAND78-8813, accepted for publication in Solar Energy.

A-1 Hoerner, S. F., Fluid-Dynamic Drag, Brick Town, N.J.: Hoerner Fluid Dynamics, 1965, pp. 4-1.

A-2 Delameter, W. R. Personal Communication, Sandia Laboratories, Livermore, CA, March 1979.

A-3 Randall, D. E., et al., "Steady State Wind Loading on Parabolic-Trough Solar Collectors," Sandia Laboratories, SAND79-2134, August, 1980.

A-4 Bergeron, K. D. et al., "Line-Focus Solar Thermal Energy Technology Development, FY79 Annual Report for Department 4720," Sandia Laboratories Report SAND80-0865, April 1980.

A-5 "Wind Forces on Structures," Paper 3269, Transactions ASCE, Vol. 126, Part II, 1961, pp. 1124-1198 (Reprinted 1972).

A-6 Sachs, Peter, Wind Forces in Engineering, Second Edition, Pergamon Press, New York, 1978.

A-7 Cermak, J. E., et al., "Heliostat Field-Array Wind-Tunnel Test," Fluid Mechanics and Wind Engineering Program Report, Colorado State University, Fort Collins, Colorado, July 1978.

A-8 Hoerner, op. cit. A-1, pp. 3-15, 16.

A-9 Bergeron, op. cit. A-4, p. 42.

A-10 "Solar Total Energy Large-Scale Experiment at Shenandoah, Georgia," Preliminary Design, Final Report, General Electric Report 78-SDS-4243, September 1978, pp. 3-48.

A-11 Sachs, op. cit. A-6, p. 294.

A-12 Hoerner, op. cit. A-1, p. 20-2.

A-13 Easton, C. R., "Solar Central Receiver Prototype Heliostat CDRL Item B.d," McDonnell Douglas Astronautics Co. Report No. MDC G7399, August 1978.

A-14 Roark, R. J., and Young, W. C., Formulas for Stress and Strain, Fifth Edition, McGraw-Hill, 1975, p. 209.

A-15 Ibid., p. 555.

A-16 Schwartz, A., Calculus and Analytic Geometry, Second Edition, Holt, Rinehart, Winston, New York, 1967, p. 685.

A-17 Perry, J. H. et al., Chemical Engineer's Handbook, Fourth Edition, McGraw Hill, New York, p. 2-6.

A-18 Bergeron, op. cit. A-4, p. 45.

A-19 1975 Morse Chain Catalogue.

A-20 Perry, op. cit. A-17, p. 26-20.

A-21 Baumeister, T., et al. (Editors), Marks' Standard Handbook for Mechanical Engineers, Eighth Edition, McGraw Hill, New York, 1978, pp. 12-46 to 12-62.

A-22 Merritt, F. S., (Editor), Standard Handbook for Civil Engineers, Second Edition, McGraw Hill, New York, 1978, Chapters 7 and 8.

A-23 Gaylord, E. H., Jr., and Gaylord, C. N., ed., Structural Engineering Handbook, Second Ed., McGraw Hill, 1979, pp. 5-81.

A-24 Dunder, V. D., Personal Communication, Sandia Laboratories, Livermore, CA, March 1979.

A-25 Clough, D., and Mettler, A., Personal Communication, ABAM Corp., Tacoma, WA, March 1979.

B-1 Hicks, T. G., ed., Standard Handbook of Engineering Calculations, McGraw-Hill, New York, NY, 1972, pp. 4-31.

INITIAL DISTRIBUTION

UNLIMITED RELEASE

U. S. Department of Energy
Albuquerque Operations Office
P. O. Box 5400
Albuquerque, NM 87185
Attn: H. Roser
J. Weisiger
G. Pappas
J. Morley
D. Schuler

U. S. Department of Energy
600 E Street NW
Washington, D. C. 20585
Attn: J. Easterling
G. W. Braun
C. Draffin
M. U. Gutstein
B. Hochheiser
M. J. Katz
L. Melamed
J. E. Rannels
W. Auer
L. Levine

U. S. Department of Energy
San Francisco Operations Office
1333 Broadway
Oakland, CA 94612
Attn: R. W. Hughey
J. LaGrone

Aerospace Corporation
Solar Thermal Projects
Energy Systems Group, D-5
Room 1110
P. O. Box 92957
El Segundo, CA 90009
Attn: P. deRienzo
P. Mathur

ARCO
911 Wilshire Blvd
Los Angeles, CA 90017
Attn: J. H. Caldwell, Jr.

Battelle PNL
P. O. Box 999
Richland, WA 99352
Attn: K. Drumheller
W. W. Laity

Bechtel National, Inc.
P. O. Box 3965
San Francisco, CA 94119
Attn: E. Lam

Black & Veatch
P. O. Box 8405
Kansas City, MO 64114
Attn: C. Grosskreutz

Chevron Research
P. O. Box 1627
Richmond, CA 94804
Attn: L. Fraas

Chevron Oil Research
P. O. Box 446
La Habra, CA 90631
Attn: W. Peake
For: J. Ploeg
W. Stiles

Electric Power Research Institute
P. O. Box 10412
Palo Alto, CA 93403
Attn: J. Bigger

Exxon Enterprises-Solar Thermal Systems
P. O. Box 592
Florham Park, NJ 07932
Attn: P. Joy
For: D. Nelson
G. Yenetchi
C. Grebenstein

Failure Analysis Associates
750 Welch Road
Palo Alto, CA 93404
Attn: E. Eason

Institute of Gas Technology
Suite 218
1825 K Street, NW
Washington, D. C. 25006
Attn: D. R. Glenn

Jet Propulsion Laboratory
Building 520-201
4800 Oak Grove Drive
Pasadena, CA 91103
Attn: T. Fujita
V. Truscello
J. Sheldon

Lawrence Livermore National Laboratory
P. O. Box 808
Livermore, CA 94550
Attn: C. J. Anderson
A. B. Casamajor
W. C. Dickinson

Los Alamos National Laboratory
P. O. Box 1663
Los Alamos, NM 87545
Attn: F. Finch
For: D. Freiwald
K. Williamson
D. Balcomb

Martin Marietta Corporation
P. O. Box 179
Denver, CO 80201
Attn: C. Bolton
A. E. Hawkins
T. Heaton
J. Montague
H. C. Wroton
T. Tracey

McDonnell Douglas Astronautics Co.
5301 Bolsa Avenue
Huntington Beach, CA 92647
Attn: P. Drummond
R. Hallet
R. Gervais
L. Weinstein

Phillips Chemical Co.
13-D2 Phillips Building
Bartlesville, OK 74004
Attn: M. Bowman

Solar Energy Research Institute
1617 Cole Boulevard
Golden, CO 80401
Attn: A. Rabl
R. Copeland
L. Dunham, TID
D. Feasby
J. Finegold
B. Gupta
F. Herlevich
D. Hooker
D. Kearney
R. Ortiz, SEIDB
J. Thornton
K. Touryan
N. Woodley

Solar Thermal Test Facility
User Association
Suite 1205
First National Bank East
Albuquerque, NM 87112
Attn: F. Smith

Southern California Edison
P. O. Box 800
Rosemead, CA 91770
Attn: Joe Reeves

Standard Oil of California
555 Market Street
San Francisco, CA 94105
Attn: S. Kleespies

C. J. Swet
Route 4 Box 258
Mt. Airy, MD 21771

University of Houston
Solar Energy Laboratory
4800 Calhoun
Houston, TX 77004
Attn: A. F. Hildebrandt
For: K. Y. Lee
E. C. Tacker
L. L. Vant-Hull

Energy Systems Group
Rockwell International
8900 DeSoto Ave.
Canoga Park, CA 91304
Attn: T. Springer

US Water & Power Resources Service
Bureau of Reclamation
Code 1500 E
Denver Federal Center
P. O. Box 25007
Denver, CO 80225
Attn: S. J. Hightower

Westinghouse Electric Corp.
700 Braddock Ave.
MS8L42
East Pittsburgh, PA 15112
Attn: J. Day

M. Sparks, 1
A. Narath, 4000; Attn: J. Scott, 4700
G. Brandvold, 4710

B. Marshall, 4713
J. F. Banas, 4716
J. A. Leonard, 4717; Attn: K. Bergeron
W. P. Schimmel, 4723; Attn: T. Dellin
T. B. Cook, 8000; Attn: A. N. Blackwell, 8200
W. J. Spencer, 8100; Attn: J. Barham, 8110
W. Alzheimer, 8120
J. Wirth, 8150
R. Cozine, 8160
H. Witek, 8115
J. B. Woodard, 8115
C. S. Hoyle, 8122
R. J. Gallagher, 8124
R. L. Rinne, 8320
C. T. Yokomizo, 8326
B. F. Murphey, 8300; Attn: D. M. Schuster, 8310
G. W. Anderson, 8330
W. Bauer, 8340
D. Hartley, 8350
J. E. Struve, 8324
J. D. Hankins, 8324
L. D. Brandt, 8326
L. Hostetler, 8328
J. J. Iannucci, 8328 (10)
C. F. Melius, 8343
L. Gutierrez, 8400; Attn: R. A. Baroody, 8410
D. E. Gregson, 8440
C. M. Tapp, 8460
C. S. Selvage, 8420
R. C. Wayne, 8450
P. J. Eicker, 8451 (50)
A. C. Skinrood, 8452
W. G. Wilson, 8453
Publications Division, 8265, for TIC (2)
Publications Division, 8265/Technical Library Processes and Systems Division, 3141
Technical Library Processes and Systems Division, 3141 (2)
M. A. Pound, 8214 for Central Technical File (3)

Org.	Bldg.	Name	Rec'd by *	Org.	Bldg.	Name	Rec'd by *

* Recipient must initial on classified documents.